

Buffon-Laplace Needle Problem with objects of arbitrary size in two and three dimensions

Yan-Jie Min,^{*} De-Quan Zhu,^{*} and Jin-Hua Zhao[†]

School of Data Science and Engineering, South China Normal University, Shanwei 516622, China

(Dated: June 19, 2024)

Buffon-Laplace Needle Problem considers a needle of a length l randomly dropped on a large plane with vertically parallel lines with distances a and b ($a \geq b$), respectively. As a classical problem in stochastic probability, it serves as a mathematical basis of various physical literature. Yet its potential application is limited by previous focus on its original form of the ‘short’ needle case of $l < b$. Here, rather than a ‘short’ two-dimensional needle, we analytically solve the problems with two- and three-dimensional needles and spherocylinders of arbitrary length and radius dropped on a grid with any rectangular shape. We further confirm our analytical theory with Monte Carlo simulation. Our framework here helps to extend the analytical power of the needle problem into unexplored parameter regions for various physical problems involving stochastic processes.

I. INTRODUCTION

Buffon-Laplace Needle Problem (BLNP) [1, 2] is one of the oldest problems in geometrical probability dated back more than two centuries. BLNP considers randomly dropping a thin needle with a length l on a two-dimensional (2D) plane distributed with two sets of equidistant parallel lines with distances a and b , respectively, which are vertical to each other, and studies the statistical property of intersections between the needle and the lines. For convenience, we set $a \geq b$ in this paper. BLNP is a natural extension of Buffon’s Needle Problem (BNP) [3], which considers a similar scenario on a plane yet with a single set of parallel lines with a distance d .

The fundamental quantity for the two needle problems is the intersection probability of a needle intersecting with at least one line. For the intersection probability $P(l, d)$ with a needle length l and a line distance d in BNP, [3] and [4](page 251-252) derive its form for the ‘short’ needle case with $l < d$. [4](page 258, problem 7) also shows $P(l, d)$ for a long needle case with $l > d$. For the intersection probability $P(l, a, b)$ with a needle length l and line distances a and b in BLNP, [1, 2] and [4](page 255-257) show a prediction of the case with $l < b$. In [5], the authors further lay down an analytical form of $P(l, a, b)$ in a specific case of $a = b$ and $l > b$ (as Eq. (6) in its main text), yet with an error in a coefficient which we will show later. Another quantity pertinent to the two needle problems is the distribution of intersections, especially in the case of a long needle. For BNP, [6] shows the distribution of intersections in the case of $l > d$.

As classical models of randomness, variants based on BNP and BLNP are frequently discussed in both mathematical and physical literature. A simple variation of the problems is to generalize needles and grid lines into other geometrical objects. For BNP, a needle can be re-

placed with a planar curve [7, 8], polygons [9], a pivot needle (two needles sharing a tip) [10], and so on. Sets of parallel lines can also be generalized to parallel stripes with a finite width [11], random Cantor sets [12, 13], a line with randomly distributed dots [14], and so on. For BLNP, a needle can be extended to an ellipse [15], a spherocylinder (a rod-like shape consistent of a cylinder and two hemispherical caps on both its ends) in three-dimensional (3D) space [5], and so on. Besides, a plane in BLNP can be considered as being covered with repeated congruent triangles [4] (page 258, problem 8).

In this paper, we revisit BLNP and focus on its analytical solution of intersection probability, the most basic quantity of the problem. For the original BLNP and many of its extensions, the initial ‘short’ needle case with $l < b$ is heavily discussed in previous literature, while analytical result for the ‘long’ needle case of $l > b$ is quite limited, as far as we know. Here we solve BLNP with dropped objects as needles and spherocylinders, and derive analytical predictions of intersection probability for any object size (such as a length l for a needle or a length l and a radius $\sigma/2$ for a spherocylinder) and any grid shape parameters (a, b) . We have two motivations for this. The first one is mathematical, in which forcing $l < b$ is unnecessary for a theoretical model. The second one is rather physical, as parameters with any l and (a, b) represent a realistic situation when the problem serves as an approximation model in a physical context. For example, in [5], after a needle is generalized to a spherocylinder, BLNP is adopted as a model for granular particles filtering through a sieve-like grid. Setting $l > b$ and $a \neq b$, rather than forcing $l < b$ and $a = b$ in the original literature, makes possible studying new complex phenomena originated from long particles and irregular grid topology.

Our main contribution in this paper is as follows: with a single probabilistic analytical framework, we calculate the intersection probability when the dropped objects are needles with no volume and spherocylinders with finite volume in both 2D and 3D spaces. Our framework naturally retrieves the equation for BLNP with ‘short’ 2D needles. Our theoretical work further helps to release the potential of BLNP as a mathematical model in various

^{*} These authors contributed equally to this work.

[†] zhaojh@m.scnu.edu.cn

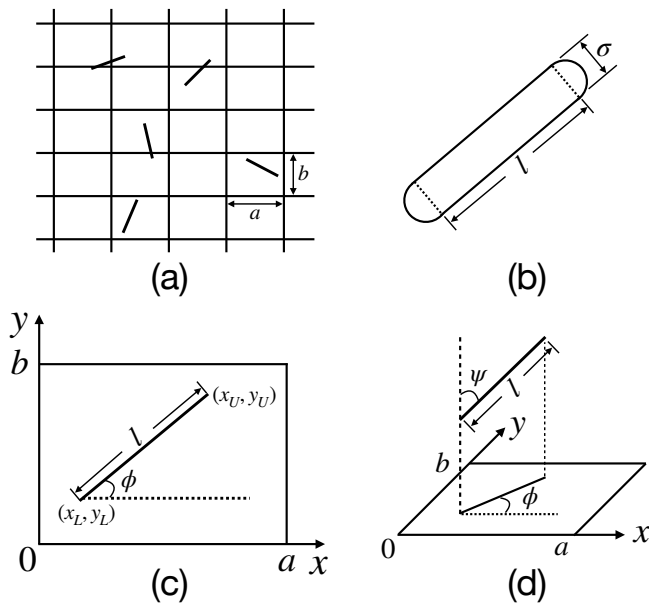


FIG. 1. BLNP with needles and spherocylinders in 2D and 3D spaces. (a) In the original BLNP with 2D needles, two sets of vertically parallel lines have distances of a and b , respectively, which form a grid. The five line segments scattered in the grid represent thin needles, three of which intersect with lines of the grid. (b) A 2D spherocylinder has a rectangle with a width l and two semicircles with a radius $\sigma/2$ on both its ends. (c) In the BLNP with 2D needles, the relative position of a needle within a grid cell with a width a and a height b is shown. The coordinates (x_U, y_U) and (x_L, y_L) represent respectively the upper and the lower tips of the needle, and the orientation $\phi \in [0, \pi)$ is the angle between the needle and the x -axis. (d) In the BLNP with 3D needles, a 3D needle is first projected onto a grid. The orientation $\psi \in [0, \pi/2]$ is the angle between the needle and a direction vertical to the grid plane. The relative position of a projected needle in a grid cell shares a similar description as in the case of 2D needles shown in (c).

physical problems.

Here is the layout of the paper. In Section II, we present BLNP and its four versions, and also lay down their representation and realization in simulation. In Sections III to VI, we explain the analytical framework to calculate the intersection probability when 2D needles, 2D spherocylinders, 3D needles, and 3D spherocylinders, respectively, are dropped on a 2D grid. In Section VII, we show our theoretical results, verified with Monte Carlo simulation. In Section VIII, we conclude the paper with some discussion.

II. MODEL

In the original BLNP, the grid is 2D with two vertical set of parallel lines, and the needle is dropped on the plane. See Fig.1(a) for an example. For convenience, we

call this type of needles as 2D ones. In this paper, we keep the grid as 2D and generalize the dropped object from a 2D needle into two directions. We first generalize a thin needle with no volume into a rod-like shape with a finite volume. This generalization makes possible consideration of real-world objects in a mathematical model. A spherocylinder [5] is intrinsically a 3D object, and consists of a cylinder with a length l and two semi-spheres with a radius $\sigma/2$ on both its ends. Due to the simple topology of its contour, the projection of a spherocylinder on a 2D plane correspondingly consists of a rectangle with a width $\leq l$ and two semicircles with a radius $\sigma/2$ on both its ends. See Fig.1(b) for an example. For simplicity, we name the original spherocylinder and its 2D projection as a 3D and a 2D spherocylinder respectively. We then generalize the embedded space of dropped objects from 2D to 3D, during which an extra degree of freedom is introduced for the objects. Beware that, an intersection between a 3D object and a 2D grid is defined between the projection of the 3D object onto the grid plane and the grid lines. Due to their simple topology, a 3D needle is projected into a 2D one, and a 3D spherocylinder is projected into a 2D one.

Summing up the above generalizations of BLNP, we consider here its four versions: (1) BLNP with 2D needles, which is simply the original BLNP; (2) BLNP with 2D spherocylinders; (3) BLNP with 3D needles; and (4) BLNP with 3D spherocylinders.

We further lay down how to perform simulation for these four versions. To count the intersection events, it is only relevant to distinguish whether or not a dropped object intersects with sets of lines, which only involves the relative position between them. Thus the picture of an object dropped on a grid with an infinitely large number of cells can be simplified into one in which an object is dropped on a single grid cell. We choose parallel lines with distances b and a to establish x - and y -axes, respectively, and then consider the relative position of a dropped object in a grid cell. As a needle and a spherocylinder both have simple geometrical boundaries, we can use only a limited number of parameters, for example coordinates of their two tips, to describe their overall positions. A general Monte Carlo simulation[16] of an object-dropping experiment can be carried out as follows: with given sizes of objects and grid cells (l, a, b) or (l, σ, a, b) , we first generate a large number N_{all} of object configurations with a pseudo-random number generator, say $\text{Rand}()$, which generates a sequence of real numbers $\in (0, 1)$ obeying a uniform distribution; we then count the number N_{coll} of configurations in which an object overlaps with at least one boundary of a grid cell; finally, we calculate the empirical intersection probability as $N_{\text{coll}}/N_{\text{all}}$.

In the above simulation process, only the description of an object configuration and the condition for an intersection vary in the four problem versions. For a 2D needle and spherocylinder, their descriptions of relative positions share a similar form and consist of three ingre-

dients: the coordinate x_U on x -axis and the coordinate y_U on y -axis for the upper tip of a needle or the center of the upper semicircle of a spherocylinder, and the orientation ϕ between a needle or a spherocylinder and the x -axis. The ‘upper’ tip or semicircle here corresponds to the one of tips or semicircles with a larger coordinate on the y -axis. Fig.1(c) shows an example for a 2D needle. The ranges of (x_U, y_U, ϕ) are $[0, a)$, $[0, b)$, and $[0, \pi)$, respectively. In a single experiment, a random configuration of a 2D needle or spherocylinder can be generated as

$$\begin{bmatrix} x_U \\ y_U \\ \phi \end{bmatrix} = \begin{bmatrix} a \times \text{Rand}() \\ b \times \text{Rand}() \\ \pi \times \text{Rand}() \end{bmatrix}. \quad (1)$$

Correspondingly, the coordinates of the lower tip of the needle or the center of the lower semicircle of the spherocylinder are

$$\begin{bmatrix} x_L \\ y_L \end{bmatrix} = \begin{bmatrix} x_U - l \cos \phi \\ y_U - l \sin \phi \end{bmatrix}. \quad (2)$$

For the description of a 3D needle or spherocylinder, except from the parameters (x_U, y_U, ϕ) , a fourth parameter $\psi \in [0, \pi/2]$ is introduced to account the orientation between an object and the axis vertical to the grid plane. See Fig.1 (d) for an example of a 3D needle. To generate a random configuration of a 3D needle or spherocylinder, we have

$$\begin{bmatrix} x_U \\ y_U \\ \psi \\ \phi \end{bmatrix} = \begin{bmatrix} a \times \text{Rand}() \\ b \times \text{Rand}() \\ \frac{\pi}{2} \times \text{Rand}() \\ \pi \times \text{Rand}() \end{bmatrix}. \quad (3)$$

Correspondingly, the coordinates of the lower tip of the 3D needle or the center of the lower semicircle of the spherocylinder of their projected shapes are respectively

$$\begin{bmatrix} x_L \\ y_L \end{bmatrix} = \begin{bmatrix} x_U - l \sin \psi \cos \phi \\ y_U - l \sin \psi \sin \phi \end{bmatrix}. \quad (4)$$

Then we consider the condition for an intersection between a dropped object and a grid cell. An intersection

between a 2D needle and the grid happens simply when at least one tip is out of the grid cell. We can state as

$$\begin{aligned} & (x_L < 0) \vee (a < x_L) \\ \vee & (y_L < 0) \vee (b < y_L), \end{aligned} \quad (5)$$

in which \vee is a logical OR operator. Beware that, in the numerical simulation with continuous real numbers, we ignore the cases when the two needle tips fall exactly on any boundary of a grid cell (say, $x = 0$ and a , and $y = 0$ and b), since their probability is infinitesimal.

To account an intersection between a 2D spherocylinder and a grid cell, the contour of a spherocylinder should be taken into consideration. It is easy to find that, an intersection happens when at least one of the furthest tips in four directions of the contour of a spherocylinder is out of a grid cell. We have the following condition as

$$\begin{aligned} & \left(x_U - \frac{\sigma}{2} < 0\right) \vee \left(a < x_U + \frac{\sigma}{2}\right) \\ \vee & \left(y_U - \frac{\sigma}{2} < 0\right) \vee \left(b < y_U + \frac{\sigma}{2}\right) \\ \vee & \left(x_L - \frac{\sigma}{2} < 0\right) \vee \left(a < x_L + \frac{\sigma}{2}\right) \\ \vee & \left(y_L - \frac{\sigma}{2} < 0\right) \vee \left(b < y_L + \frac{\sigma}{2}\right). \end{aligned} \quad (6)$$

When the line distance $a \rightarrow \infty$, the constraint from parallel lines along the y -axis vanishes, and two sets of parallel lines effectively reduce to only one set. In this case, the BLNP with 2D needles, 2D spherocylinders, 3D needles, and 3D spherocylinders reduce to its BNP versions, respectively. For the simulation of four BNP versions, we can simply remove x_U and x_L from the description of object configuration in Eqs.(1)-(4), along with those terms with x_U and x_L in Eqs.(5) and (6).

Based on the above representations of the relative position of an object dropped on a grid, we further develop a consistent analytical framework to calculate the intersection probability with any size of objects and grid cells. In the following four sections, starting from the original BLNP version with 2D needles, we theoretically solve problems with increasing complexity until the one with 3D spherocylinders. Furthermore, by setting $1/a \rightarrow 0$, these theoretical equations naturally reduce to those for the four BNP versions, respectively.

III. THEORY OF BLNP WITH 2D NEEDLES

To compute the intersection probability for the four BLNP versions, our basic logic is to navigate in the parameter space of configurations of a dropped object in a grid cell and calculate the fraction of the volume of parameter space, in which an intersection happens, among the total volume of the parameter space.

Specifically, for the BLNP with 2D needles, we calculate two volumes: S_{all} as one of the total parameter space of (x_U, y_U, ϕ) for a needle configuration, and S_{coll} as one of the proper parameter space of (x_U, y_U, ϕ) which results in

an intersection between the needle and the grid cell. The intersection probability $P(l, a, b)$ can be formulated as

$$P(l, a, b) = \frac{S_{\text{coll}}}{S_{\text{all}}}. \quad (7)$$

It is easy to find that

$$S_{\text{all}} = ab\pi. \quad (8)$$

The challenging part here is to derive an explicit form for S_{coll} . We reformulate S_{coll} as

$$S_{\text{coll}} = S_{\text{coll}}(x) + S_{\text{coll}}(y) - S_{\text{coll}}(x, y), \quad (9)$$

in which $S_{\text{coll}}(x)$, $S_{\text{coll}}(y)$, and $S_{\text{coll}}(x, y)$ denote the volume of the parameter space of (x_U, y_U, ϕ) when an intersection between a 2D needle and a grid cell happens on the boundaries of the grid cell along the y -axis (say, $x = 0$ and a), the x -axis (say, $y = 0$ and b), and the x - and y -axes at the same time, respectively. Based on Eqs.(1), (2), and (5), we have

$$\begin{aligned} S_{\text{coll}}(x) &= \int_0^{\frac{\pi}{2}} d\phi \int_0^a \Theta(l \cos \phi - x) dx \int_0^b dy + \int_{\frac{\pi}{2}}^{\pi} d\phi \int_0^a \Theta(-l \cos \phi + x - a) dx \int_0^b dy \\ &= b \int_0^{\frac{\pi}{2}} d\phi \int_0^a \Theta(l \cos \phi - x) dx + b \int_{\frac{\pi}{2}}^{\pi} d\phi \int_0^a \Theta(-l \cos \phi - x) dx \\ &= b \int_0^{\pi} d\phi \int_0^a \Theta(|l \cos \phi| - x) dx, \end{aligned} \quad (10)$$

$$\begin{aligned} S_{\text{coll}}(y) &= \int_0^{\pi} d\phi \int_0^a dx \int_0^b \Theta(l \sin \phi - y) dy \\ &= a \int_0^{\pi} d\phi \int_0^b \Theta(l \sin \phi - y) dy, \end{aligned} \quad (11)$$

$$\begin{aligned} S_{\text{coll}}(x, y) &= \int_0^{\frac{\pi}{2}} d\phi \int_0^a \Theta(l \cos \phi - x) dx \int_0^b \Theta(l \sin \phi - y) dy + \int_{\frac{\pi}{2}}^{\pi} d\phi \int_0^a \Theta(-l \cos \phi + x - a) dx \int_0^b \Theta(l \sin \phi - y) dy \\ &= \int_0^{\frac{\pi}{2}} d\phi \int_0^a \Theta(l \cos \phi - x) dx \int_0^b \Theta(l \sin \phi - y) dy + \int_{\frac{\pi}{2}}^{\pi} d\phi \int_0^a \Theta(-l \cos \phi - x) dx \int_0^b \Theta(l \sin \phi - y) dy \\ &= \int_0^{\pi} d\phi \int_0^a \Theta(|l \cos \phi| - x) dx \int_0^b \Theta(l \sin \phi - y) dy. \end{aligned} \quad (12)$$

In the above integrals, we denote (x, y) for (x_U, y_U) for convenience. The step function $\Theta(x)$ is defined as $\Theta(x) = 1$ if $x \geq 0$ and 0 otherwise. Combining a step function with the integrands on the parameters (x_U, y_U, ϕ) singles out proper ranges which permit an intersection between a needle and a grid cell. On the righthand side of the second equal signs of Eqs.(10) and (12), with a change of variables as $x - a \rightarrow -\hat{x}$, we have

$$\begin{aligned} \int_0^a \Theta(-l \cos \phi + x - a) dx &= \int_a^0 \Theta(-l \cos \phi - \hat{x}) d(-\hat{x}) \\ &= \int_0^a \Theta(-l \cos \phi - \hat{x}) d\hat{x}. \end{aligned} \quad (13)$$

An alternative way to calculate S_{coll} is

$$S_{\text{coll}} = S_{\text{all}} - S_{\text{non-coll}}, \quad (14)$$

in which $S_{\text{non-coll}}$ is the volume of the parameter space of (x_U, y_U, ϕ) where there is no intersection between a needle and a grid cell. Following the same logic in Eqs.(10)-(12), we have

$$\begin{aligned} S_{\text{non-coll}} &= \int_0^{\frac{\pi}{2}} d\phi \int_0^a \Theta(x - l \cos \phi) dx \int_0^b \Theta(y - l \sin \phi) dy + \int_{\frac{\pi}{2}}^{\pi} d\phi \int_0^a \Theta(x + l \cos \phi) dx \int_0^b \Theta(y - l \sin \phi) dy \\ &= \int_0^{\pi} d\phi \int_0^a \Theta(x - |l \cos \phi|) dx \int_0^b \Theta(y - l \sin \phi) dy. \end{aligned} \quad (15)$$

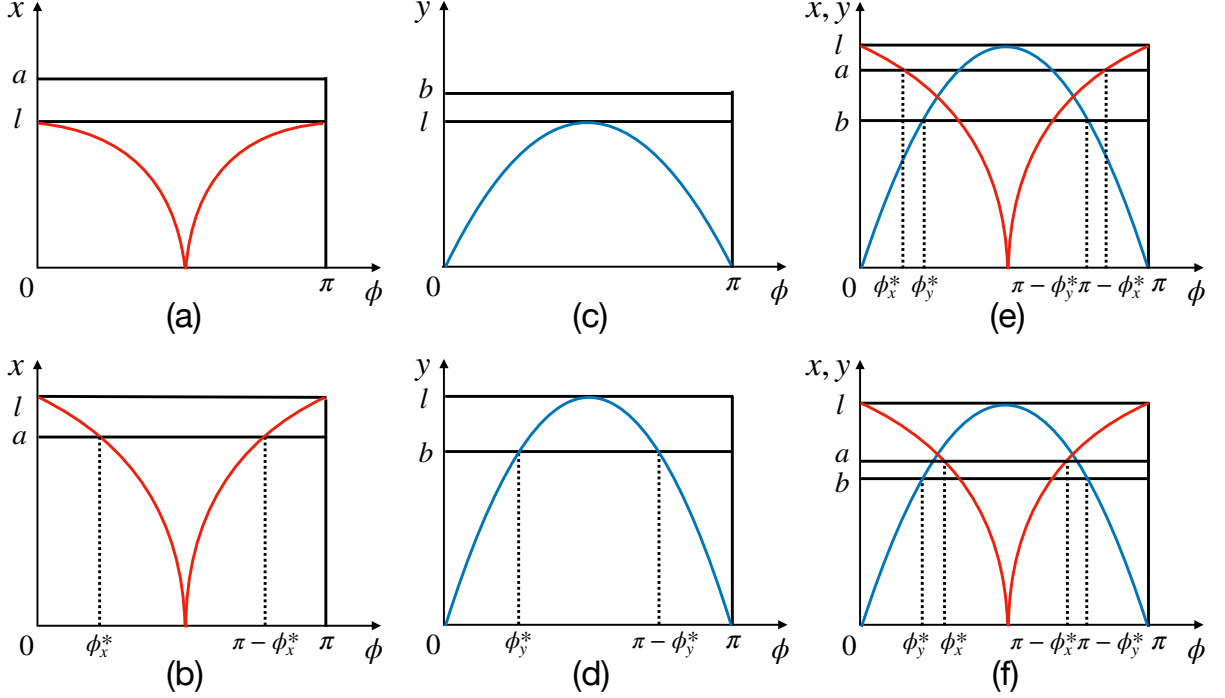


FIG. 2. Relative sizes among l , a , and b . (a)-(b) The curve $x = |l \cos \phi|$ is shown under the conditions of $l \leq a$ and $a < l$, respectively. $\phi_x^* \in (0, \pi/2)$ and $\pi - \phi_x^*$ are the ϕ -coordinates at which the lines $x = |l \cos \phi|$ and $x = a$ overlap. (c)-(d) The curve $y = l \sin \phi$ is shown under the conditions of $l \leq b$ and $b < l$, respectively. $\phi_y^* \in (0, \pi/2)$ and $\pi - \phi_y^*$ are the ϕ -coordinates at which the lines $y = l \sin \phi$ and $y = b$ overlap. (e)-(f) The curves $x = |l \cos \phi|$ and $y = l \sin \phi$ are shown at the same time under the conditions of $\phi_x^* \leq \phi_y^*$, equivalently $l \leq \sqrt{a^2 + b^2}$, and $\phi_y^* < \phi_x^*$, equivalently $\sqrt{a^2 + b^2} < l$, respectively.

We should mention that these two frameworks to calculate S_{coll} are equivalent. Yet the former is more direct in computation, which we will follow in this paper.

Before our detailed calculation, we define some integrals from above equations as

$$A(l, a) \equiv \int_0^\pi d\phi \int_0^a \Theta(|l \cos \phi| - x) dx, \quad (16)$$

$$B(l, b) \equiv \int_0^\pi d\phi \int_0^b \Theta(l \sin \phi - y) dy, \quad (17)$$

$$AB(l, a, b) \equiv \int_0^\pi d\phi \int_0^a \Theta(|l \cos \phi| - x) dx \int_0^b \Theta(l \sin \phi - y) dy. \quad (18)$$

Correspondingly, we rewrite S_{coll} as

$$S_{\text{coll}} = bA(l, a) + aB(l, b) - AB(l, a, b). \quad (19)$$

We can easily find that

$$\int_0^a \Theta(|l \cos \phi| - x) dx = \min\{|l \cos \phi|, a\}, \quad (20)$$

$$\int_0^b \Theta(l \sin \phi - y) dy = \min\{l \sin \phi, b\}. \quad (21)$$

To finish the computation of Eqs.(16)-(18), we should examine the relative sizes among l , a , and b , which are shown schematically in Fig.2. We write $A(l, a)$ in the case of $l \leq a$ and $a < l$ respectively as $A(l, a|l \leq a)$ and $A(l, a|a < l)$. When $l \leq a$, $|l \cos \phi| \leq a$ always holds for $\phi \in [0, \pi)$. Yet when $a < l$, $|l \cos \phi| \leq a$ holds only when $\phi \in [\phi_x^*, \pi - \phi_x^*]$, in which we define

$$\phi_x^* = \arccos \frac{a}{l}. \quad (22)$$

See Fig.2 (a) and (b) for an illustration. We have

$$\begin{aligned} A(l, a|l \leq a) &= \int_0^{\frac{\pi}{2}} d\phi \cdot l \cos \phi + \int_{\frac{\pi}{2}}^{\pi} d\phi \cdot (-l \cos \phi) \\ &= 2l, \end{aligned} \quad (23)$$

$$\begin{aligned} A(l, a|a < l) &= \int_0^{\phi_x^*} d\phi \cdot a + \int_{\phi_x^*}^{\frac{\pi}{2}} d\phi \cdot l \cos \phi + \int_{\frac{\pi}{2}}^{\pi - \phi_x^*} d\phi \cdot (-l \cos \phi) + \int_{\pi - \phi_x^*}^{\pi} d\phi \cdot a \\ &= 2l(1 - \sin \phi_x^*) + 2a\phi_x^*. \end{aligned} \quad (24)$$

We then write $B(l, b)$ in the case of $l \leq b$ and $b < l$ respectively as $B(l, b|l \leq b)$ and $B(l, b|b < l)$. When $l \leq b$, $l \sin \phi \leq b$ always holds for $\phi \in [0, \pi)$. Yet when $b < l$, $l \sin \phi \leq b$ holds only when $\phi \in [0, \phi_y^*] \cup [\pi - \phi_y^*, \pi)$, in which we define

$$\phi_y^* = \arcsin \frac{b}{l}. \quad (25)$$

See Fig.2 (c) and (d) for an illustration. We have

$$\begin{aligned} B(l, b|l \leq b) &= \int_0^{\pi} d\phi \cdot l \sin \phi \\ &= 2l, \end{aligned} \quad (26)$$

$$\begin{aligned} B(l, b|b < l) &= \int_0^{\phi_y^*} d\phi \cdot l \sin \phi + \int_{\phi_y^*}^{\pi - \phi_y^*} d\phi \cdot b + \int_{\pi - \phi_y^*}^{\pi} d\phi \cdot l \sin \phi \\ &= 2l(1 - \cos \phi_y^*) + 2b \left(\frac{\pi}{2} - \phi_y^* \right). \end{aligned} \quad (27)$$

To calculate $AB(l, a, b)$ and finally $P(l, a, b)$, the relative sizes among (l, a, b) are more involved. We will detail four cases below.

A. The case of $l \leq b$

We write $AB(l, a, b)$ when $l \leq b$ as $AB(l, a, b|l \leq b)$. With Eq.(18) we have

$$\begin{aligned} AB(l, a, b|l \leq b) &= \int_0^{\frac{\pi}{2}} d\phi \cdot l \cos \phi \cdot l \sin \phi + \int_{\frac{\pi}{2}}^{\pi} d\phi \cdot (-l \cos \phi) \cdot l \sin \phi \\ &= l^2. \end{aligned} \quad (28)$$

With Eq.(19) we then have

$$\begin{aligned} S_{\text{coll}} &= bA(l, a|l \leq a) + aB(l, b|l \leq b) - AB(l, a, b|l \leq b) \\ &= 2lb + 2la - l^2. \end{aligned} \quad (29)$$

We thus have

$$P(l, a, b) = \frac{2}{\pi} \left(\frac{l}{a} + \frac{l}{b} \right) - \frac{1}{\pi} \frac{l^2}{ab}. \quad (30)$$

Here we simply retrieve the result for the ‘short’ needle case of $l < b$ in [1, 2].

B. The case of $b < l \leq a$

We write $AB(l, a, b)$ when $b < l \leq a$ as $AB(l, a, b|b < l \leq a)$. We have

$$\begin{aligned} AB(l, a, b|b < l \leq a) &= \int_0^{\phi_y^*} d\phi \cdot l \cos \phi \cdot l \sin \phi + \int_{\phi_y^*}^{\frac{\pi}{2}} d\phi \cdot l \cos \phi \cdot b \\ &\quad + \int_{\frac{\pi}{2}}^{\pi - \phi_y^*} d\phi \cdot (-l \cos \phi) \cdot b + \int_{\pi - \phi_y^*}^{\pi} d\phi \cdot (-l \cos \phi) \cdot l \sin \phi \\ &= 2lb - b^2. \end{aligned} \quad (31)$$

Then,

$$\begin{aligned}
S_{\text{coll}} &= bA(l, a|l \leq a) + aB(l, b|b < l) - AB(l, a, b|b < l \leq a) \\
&= b^2 + 2la(1 - \cos \phi_y^*) + 2ab \left(\frac{\pi}{2} - \phi_y^* \right) \\
&= b^2 + 2la \left(1 - \sqrt{1 - \frac{b^2}{l^2}} \right) + 2ab \left(\frac{\pi}{2} - \arcsin \frac{b}{l} \right).
\end{aligned} \tag{32}$$

We thus have

$$P(l, a, b) = \frac{1}{\pi} \frac{b}{a} + \frac{2}{\pi} \frac{l}{b} \left(1 - \sqrt{1 - \frac{b^2}{l^2}} \right) + \frac{2}{\pi} \left(\frac{\pi}{2} - \arcsin \frac{b}{l} \right). \tag{33}$$

C. The cases in $a < l$

To further calculate $AB(l, a, b)$, we should check the relative size between ϕ_x^* and ϕ_y^* . When $a < l \leq L$ as we define $L \equiv \sqrt{a^2 + b^2}$, we have $1 - a^2/l^2 \leq b^2/l^2$. Equivalently we have $\sin^2 \phi_x^* \leq \sin^2 \phi_y^*$, correspondingly $\phi_x^* \leq \phi_y^*$. See Fig.2 (e) for an illustration. Here we write $AB(l, a, b)$ when $a < l \leq L$ as $AB(l, a, b|a < l \leq L)$. We have

$$\begin{aligned}
AB(l, a, b|a < l \leq L) &= \int_0^{\phi_x^*} d\phi \cdot a \cdot l \sin \phi + \int_{\phi_x^*}^{\phi_y^*} d\phi \cdot l \cos \phi \cdot l \sin \phi + \int_{\phi_y^*}^{\frac{\pi}{2}} d\phi \cdot l \cos \phi \cdot b \\
&+ \int_{\frac{\pi}{2}}^{\pi - \phi_y^*} d\phi \cdot (-l \cos \phi) \cdot b + \int_{\pi - \phi_y^*}^{\pi - \phi_x^*} d\phi \cdot (-l \cos \phi) \cdot l \sin \phi + \int_{\pi - \phi_x^*}^{\pi} d\phi \cdot a \cdot l \sin \phi \\
&= 2la + 2lb - L^2 - l^2.
\end{aligned} \tag{34}$$

Then,

$$\begin{aligned}
S_{\text{coll}} &= bA(l, a|a < l) + aB(l, b|b < l) - AB(l, a, b|a < l \leq L) \\
&= L^2 + l^2 - 2lb \sin \phi_x^* - 2la \cos \phi_y^* + 2ab \left(\phi_x^* + \frac{\pi}{2} - \phi_y^* \right) \\
&= L^2 + l^2 - 2 \left(lb \sqrt{1 - \frac{a^2}{l^2}} + la \sqrt{1 - \frac{b^2}{l^2}} \right) + 2ab \left(\pi - \arcsin \frac{a}{l} - \arcsin \frac{b}{l} \right).
\end{aligned} \tag{35}$$

Correspondingly,

$$P(l, a, b) = \frac{1}{\pi} \left(\frac{L^2}{ab} + \frac{l^2}{ab} \right) - \frac{2}{\pi} \left(\frac{l}{a} \sqrt{1 - \frac{a^2}{l^2}} + \frac{l}{b} \sqrt{1 - \frac{b^2}{l^2}} \right) + \frac{2}{\pi} \left(\pi - \arcsin \frac{a}{l} - \arcsin \frac{b}{l} \right). \tag{36}$$

When $L < l$, we have $\phi_y^* < \phi_x^*$ equivalently. We write $AB(l, a, b)$ when $L < l$ as $AB(l, a, b|L < l)$. We have

$$\begin{aligned}
AB(l, a, b|L < l) &= \int_0^{\phi_y^*} d\phi \cdot a \cdot l \sin \phi + \int_{\phi_y^*}^{\phi_x^*} d\phi \cdot a \cdot b + \int_{\phi_x^*}^{\frac{\pi}{2}} d\phi \cdot l \cos \phi \cdot b \\
&+ \int_{\frac{\pi}{2}}^{\pi - \phi_x^*} d\phi \cdot (-l \cos \phi) \cdot b + \int_{\pi - \phi_x^*}^{\pi - \phi_y^*} d\phi \cdot a \cdot b + \int_{\pi - \phi_y^*}^{\pi} d\phi \cdot a \cdot l \sin \phi \\
&= 2la(1 - \cos \phi_y^*) + 2lb(1 - \sin \phi_x^*) + 2ab(\phi_x^* - \phi_y^*).
\end{aligned} \tag{37}$$

Then,

$$\begin{aligned}
S_{\text{coll}} &= bA(l, a|a < l) + aB(l, b|b < l) - AB(l, a, b|L < l) \\
&= ab\pi,
\end{aligned} \tag{38}$$

after most terms cancel out. Correspondingly, we have

$$P(l, a, b) = 1. \tag{39}$$

This result has a simple geometrical interpretation. The longest distance between two points in a grid cell with a width a and a height b is the diagonal line with a distance of $L(\equiv \sqrt{a^2 + b^2})$. Thus any needle with a length $l \geq L$ dropped on a grid is certain to intersect with grid lines, leading to $P(l, a, b) = 1$.

D. Summed results

Summing up the results in Eqs. (30), (33), (36), and (39), we have

$$P(l, a, b) = \begin{cases} \frac{2}{\pi} \left(\frac{l}{a} + \frac{l}{b} \right) - \frac{1}{\pi} \frac{l^2}{ab}, & \text{if } l \leq b; \\ \frac{1}{\pi} \frac{b}{a} + \frac{2}{\pi} \frac{l}{b} \left(1 - \sqrt{1 - \frac{b^2}{l^2}} \right) + \frac{2}{\pi} \left(\frac{\pi}{2} - \arcsin \frac{b}{l} \right), & \text{if } b < l \leq a; \\ \frac{1}{\pi} \left(\frac{L^2}{ab} + \frac{l^2}{ab} \right) - \frac{2}{\pi} \left(\frac{l}{a} \sqrt{1 - \frac{a^2}{l^2}} + \frac{l}{b} \sqrt{1 - \frac{b^2}{l^2}} \right) \\ + \frac{2}{\pi} \left(\pi - \arcsin \frac{a}{l} - \arcsin \frac{b}{l} \right), & \text{if } a < l \leq L; \\ 1, & \text{if } L < l. \end{cases} \quad (40)$$

When $a \rightarrow \infty$, then $l/a \rightarrow 0$. Eqs.(30) and (33) simplify to the result for the BNP with 2D needles as

$$P(l, \infty, b) = \begin{cases} \frac{2}{\pi} \frac{l}{b}, & \text{if } l \leq b; \\ \frac{2}{\pi} \frac{l}{b} \left(1 - \sqrt{1 - \frac{b^2}{l^2}} \right) + \frac{2}{\pi} \left(\frac{\pi}{2} - \arcsin \frac{b}{l} \right), & \text{if } b < l, \end{cases} \quad (41)$$

which is just the result of the original BNP in [4].

A necessary condition for the correctness of Eq.(40) is the consistence of $P(l, a, b)$, equivalently S_{coll} , at the boundaries of the four cases of l . When $l = 0$, in the case of $l \leq b$, we have

$$S_{\text{coll}} = 0, \quad (42)$$

which is quite intuitive.

When $l = b$, both S_{coll} in the cases of $l \leq b$ and $b < l \leq a$ reduce to

$$S_{\text{coll}} = b^2 + 2ab. \quad (43)$$

When $l = a$, both S_{coll} in the cases of $b < l \leq a$ and $a < l \leq L$ reduce to

$$S_{\text{coll}} = b^2 + 2a^2 \left(1 - \sqrt{1 - \frac{b^2}{a^2}} \right) + 2ab \left(\frac{\pi}{2} - \arcsin \frac{b}{a} \right). \quad (44)$$

When $l = L$, S_{coll} in the case of $a < l \leq L$ reduces to

$$S_{\text{coll}} = ab\pi, \quad (45)$$

which equals S_{coll} in the case of $L < l$ in Eq.(38).

We further compare our equations with a previous one. The paper [5] considers a special case with $a = b = 1$, and derives the intersection probability for $b < l$ in Eq. (6) in its main text. Based on Eq.(36) here and setting $a = b = 1$, we have

$$P(l, 1, 1) = 1 - \frac{2}{\pi} \left(\arcsin \frac{1}{l} - \arccos \frac{1}{l} + 2\sqrt{l^2 - 1} - \frac{l^2}{2} - 1 \right). \quad (46)$$

We can easily find that there is an error in Eq.(6) of [5] as the coefficient $1/\pi$ of the second term should be $2/\pi$ as we show above.

IV. THEORY OF BLNP WITH 2D SPHEROCYLINDERS

Following the language in the BLNP with 2D needles, we calculate the intersection probability for the BLNP with 2D spherocylinders as

$$P(l, \sigma, a, b) = \frac{S_{\text{coll}}}{S_{\text{all}}}. \quad (47)$$

With a slight abuse of notations, we define S_{all} as the volume of total parameter space of (x_U, y_U, ϕ) , and S_{coll} as the volume of parameters space of (x_U, y_U, ϕ) which permit an intersection between a 2D spherocylinder and a grid.

Rewriting S_{coll} as Eq.(9), we define $S_{\text{coll}}(x)$, $S_{\text{coll}}(y)$, and $S_{\text{coll}}(x, y)$ here as the volume of the parameter space of (x_U, y_U, ϕ) which lead to an intersection between a 2D spherocylinder and a grid cell on the boundaries of the grid cell along the y -axis, the x -axis, and the x - and y -axes at the same time, respectively. Based on Eqs.(1), (2), and (6), and following the derivation in Eqs.(10)-(12), we have

$$\begin{aligned}
S_{\text{coll}}(x) &= \int_0^{\frac{\pi}{2}} d\phi \left[\int_0^{\frac{\sigma}{2}} dx + \int_{\frac{\sigma}{2}}^{a-\frac{\sigma}{2}} \Theta \left(l \cos \phi - x + \frac{\sigma}{2} \right) dx + \int_{a-\frac{\sigma}{2}}^a dx \right] \int_0^b dy \\
&+ \int_{\frac{\pi}{2}}^{\pi} d\phi \left[\int_0^{\frac{\sigma}{2}} dx + \int_{\frac{\sigma}{2}}^{a-\frac{\sigma}{2}} \Theta \left(-l \cos \phi + x + \frac{\sigma}{2} - a \right) dx + \int_{a-\frac{\sigma}{2}}^a dx \right] \int_0^b dy \\
&= \int_0^{\frac{\pi}{2}} d\phi \left[\int_0^{a-\sigma} \Theta (l \cos \phi - x) dx + \sigma \right] \cdot b + \int_{\frac{\pi}{2}}^{\pi} d\phi \left[\int_0^{a-\sigma} \Theta (-l \cos \phi - x) dx + \sigma \right] \cdot b \\
&= b \int_0^{\frac{\pi}{2}} d\phi \int_0^{a-\sigma} \Theta (l \cos \phi - x) dx + b \int_{\frac{\pi}{2}}^{\pi} d\phi \int_0^{a-\sigma} \Theta (-l \cos \phi - x) dx + \sigma b \pi \\
&= b \int_0^{\pi} d\phi \int_0^{a-\sigma} \Theta (|l \cos \phi| - x) dx + \sigma b \pi. \tag{48}
\end{aligned}$$

$$\begin{aligned}
S_{\text{coll}}(y) &= \int_0^{\pi} d\phi \int_0^a dx \left[\int_0^{\frac{\sigma}{2}} dy + \int_{\frac{\sigma}{2}}^{b-\frac{\sigma}{2}} \Theta \left(l \sin \phi - y + \frac{\sigma}{2} \right) dy + \int_{b-\frac{\sigma}{2}}^b dy \right] \\
&= \int_0^{\pi} d\phi \cdot a \cdot \left[\int_0^{b-\sigma} \Theta (l \sin \phi - y) dy + \sigma \right] \\
&= a \int_0^{\pi} d\phi \int_0^{b-\sigma} \Theta (l \sin \phi - y) dy + \sigma a \pi, \tag{49}
\end{aligned}$$

$$\begin{aligned}
S_{\text{coll}}(x, y) &= \int_0^{\frac{\pi}{2}} d\phi \left[\int_0^{\frac{\sigma}{2}} dx + \int_{\frac{\sigma}{2}}^{a-\frac{\sigma}{2}} \Theta \left(l \cos \phi - x + \frac{\sigma}{2} \right) dx + \int_{a-\frac{\sigma}{2}}^a dx \right] \\
&\times \left[\int_0^{\frac{\sigma}{2}} dy + \int_{\frac{\sigma}{2}}^{b-\frac{\sigma}{2}} \Theta \left(l \sin \phi - y + \frac{\sigma}{2} \right) dy + \int_{b-\frac{\sigma}{2}}^b dy \right] \\
&+ \int_{\frac{\pi}{2}}^{\pi} d\phi \left[\int_0^{\frac{\sigma}{2}} dx + \int_{\frac{\sigma}{2}}^{a-\frac{\sigma}{2}} \Theta \left(-l \cos \phi + x + \frac{\sigma}{2} - a \right) dx + \int_{a-\frac{\sigma}{2}}^a dx \right] \\
&\times \left[\int_0^{\frac{\sigma}{2}} dy + \int_{\frac{\sigma}{2}}^{b-\frac{\sigma}{2}} \Theta \left(l \sin \phi - y + \frac{\sigma}{2} \right) dy + \int_{b-\frac{\sigma}{2}}^b dy \right] \\
&= \int_0^{\frac{\pi}{2}} d\phi \left[\int_0^{a-\sigma} \Theta (l \cos \phi - x) dx + \sigma \right] \left[\int_0^{b-\sigma} \Theta (l \sin \phi - y) dy + \sigma \right] \\
&+ \int_{\frac{\pi}{2}}^{\pi} d\phi \left[\int_0^{a-\sigma} \Theta (-l \cos \phi - x) dx + \sigma \right] \left[\int_0^{b-\sigma} \Theta (l \sin \phi - y) dy + \sigma \right] \\
&= \int_0^{\pi} d\phi \left[\int_0^{a-\sigma} \Theta (|l \cos \phi| - x) dx + \sigma \right] \left[\int_0^{b-\sigma} \Theta (l \sin \phi - y) dy + \sigma \right] \\
&= \int_0^{\pi} d\phi \int_0^{a-\sigma} \Theta (|l \cos \phi| - x) dx \int_0^{b-\sigma} \Theta (l \sin \phi - y) dy \\
&+ \sigma \int_0^{\pi} d\phi \int_0^{a-\sigma} \Theta (|l \cos \phi| - x) dx + \sigma \int_0^{\pi} d\phi \int_0^{b-\sigma} \Theta (l \sin \phi - y) dy + \sigma^2 \pi. \tag{50}
\end{aligned}$$

In the above equations, we make some rearrangement in integrals with a change of variables. With $x - \frac{\sigma}{2} \rightarrow \hat{x}$, we have

$$\int_{\frac{\sigma}{2}}^{a-\frac{\sigma}{2}} \Theta \left(l \cos \phi - x + \frac{\sigma}{2} \right) dx = \int_0^{a-\sigma} \Theta (l \cos \phi - \hat{x}) d\hat{x}. \tag{51}$$

With $x + \frac{\sigma}{2} - a \rightarrow -\hat{x}$, we have

$$\begin{aligned} \int_{\frac{\sigma}{2}}^{a-\frac{\sigma}{2}} \Theta \left(-l \cos \phi + x + \frac{\sigma}{2} - a \right) dx &= \int_{a-\sigma}^0 \Theta (-l \cos \phi - \hat{x}) d(-\hat{x}) \\ &= \int_0^{a-\sigma} \Theta (-l \cos \phi - \hat{x}) d\hat{x}. \end{aligned} \quad (52)$$

With $y - \frac{\sigma}{2} \rightarrow \hat{y}$, we have

$$\int_{\frac{\sigma}{2}}^{b-\frac{\sigma}{2}} \Theta \left(l \sin \phi - y + \frac{\sigma}{2} \right) dy = \int_0^{b-\sigma} \Theta (l \sin \phi - \hat{y}) d\hat{y}. \quad (53)$$

With the definitions in Eqs. (16)-(18), we reformulate Eqs. (48)-(50) as

$$S_{\text{coll}}(x) = bA(l, a - \sigma) + \sigma b\pi, \quad (54)$$

$$S_{\text{coll}}(y) = aB(l, b - \sigma) + \sigma a\pi, \quad (55)$$

$$S_{\text{coll}}(x, y) = AB(l, a - \sigma, b - \sigma) + \sigma A(l, a - \sigma) + \sigma B(l, b - \sigma) + \sigma^2 \pi. \quad (56)$$

Correspondingly, we have

$$S_{\text{coll}} = (b - \sigma)A(l, a - \sigma) + (a - \sigma)B(l, b - \sigma) - AB(l, a - \sigma, b - \sigma) + (\sigma a + \sigma b - \sigma^2) \pi. \quad (57)$$

With the results of Eqs.(16)-(18) in Sec.III, we can directly lay down the result of Eq.(57). First, as Eqs.(22) and (25), we define here

$$\hat{\phi}_x^* = \arccos \frac{a - \sigma}{l}, \quad (58)$$

$$\hat{\phi}_y^* = \arcsin \frac{b - \sigma}{l}. \quad (59)$$

When $l \leq b - \sigma$, we have

$$\begin{aligned} S_{\text{coll}} &= (b - \sigma)A(l, a - \sigma | l \leq a - \sigma) + (a - \sigma)B(l, b - \sigma | l \leq b - \sigma) \\ &\quad - AB(l, a - \sigma, b - \sigma | l \leq b - \sigma) + (\sigma a + \sigma b - \sigma^2) \pi \\ &= 2l(b - \sigma) + 2l(a - \sigma) - l^2 + (\sigma a + \sigma b - \sigma^2) \pi. \end{aligned} \quad (60)$$

Thus,

$$P(l, \sigma, a, b) = \frac{2}{\pi} \frac{b - \sigma}{b} \frac{l}{a} + \frac{2}{\pi} \frac{a - \sigma}{a} \frac{l}{b} - \frac{1}{\pi} \frac{l^2}{ab} + \left(\frac{\sigma}{a} + \frac{\sigma}{b} - \frac{\sigma^2}{ab} \right). \quad (61)$$

When $b - \sigma < l \leq a - \sigma$, we have

$$\begin{aligned} S_{\text{coll}} &= (b - \sigma)A(l, a - \sigma | l \leq a - \sigma) + (a - \sigma)B(l, b - \sigma | b - \sigma < l) \\ &\quad - AB(l, a - \sigma, b - \sigma | b - \sigma < l \leq a - \sigma) + (\sigma a + \sigma b - \sigma^2) \pi \\ &= (b - \sigma)^2 + 2l(a - \sigma)(1 - \cos \hat{\phi}_y^*) + 2(a - \sigma)(b - \sigma) \left(\frac{\pi}{2} - \hat{\phi}_y^* \right) + (\sigma a + \sigma b - \sigma^2) \pi \\ &= (b - \sigma)^2 + 2l(a - \sigma) \left[1 - \sqrt{1 - \frac{(b - \sigma)^2}{l^2}} \right] + 2(a - \sigma)(b - \sigma) \left(\frac{\pi}{2} - \arcsin \frac{b - \sigma}{l} \right) + (\sigma a + \sigma b - \sigma^2) \pi \end{aligned} \quad (62)$$

Thus,

$$\begin{aligned} P(l, \sigma, a, b) &= \frac{1}{\pi} \frac{(b - \sigma)^2}{ab} + \frac{2}{\pi} \frac{a - \sigma}{a} \frac{l}{b} \left[1 - \sqrt{1 - \frac{(b - \sigma)^2}{l^2}} \right] \\ &\quad + \frac{2}{\pi} \frac{a - \sigma}{a} \frac{b - \sigma}{b} \left(\frac{\pi}{2} - \arcsin \frac{b - \sigma}{l} \right) + \left(\frac{\sigma}{a} + \frac{\sigma}{b} - \frac{\sigma^2}{ab} \right). \end{aligned} \quad (63)$$

If $a - \sigma < l \leq \hat{L}$ as we define $\hat{L} \equiv \sqrt{(a - \sigma)^2 + (b - \sigma)^2}$, we have $\hat{\phi}_x^* \leq \hat{\phi}_y^*$ correspondingly. Then

$$\begin{aligned}
S_{\text{coll}} &= (b - \sigma)A(l, a - \sigma | a - \sigma < l) + (a - \sigma)B(l, b - \sigma | b - \sigma < l) \\
&\quad - AB(l, a - \sigma, b - \sigma | a - \sigma < l \leq \hat{L}) + (\sigma a + \sigma b - \sigma^2) \pi \\
&= \hat{L}^2 + l^2 - 2l(b - \sigma) \sin \hat{\phi}_x^* - 2l(a - \sigma) \cos \hat{\phi}_y^* \\
&\quad + 2(a - \sigma)(b - \sigma) \left(\hat{\phi}_x^* + \frac{\pi}{2} - \hat{\phi}_y^* \right) + (\sigma a + \sigma b - \sigma^2) \pi \\
&= \hat{L}^2 + l^2 - 2l(b - \sigma) \sqrt{1 - \frac{(a - \sigma)^2}{l^2}} - 2l(a - \sigma) \sqrt{1 - \frac{(b - \sigma)^2}{l^2}} \\
&\quad + 2(a - \sigma)(b - \sigma) \left(\pi - \arcsin \frac{a - \sigma}{l} - \arcsin \frac{b - \sigma}{l} \right) + (\sigma a + \sigma b - \sigma^2) \pi.
\end{aligned} \tag{64}$$

Thus,

$$\begin{aligned}
P(l, \sigma, a, b) &= \frac{1}{\pi} \left(\frac{\hat{L}^2}{ab} + \frac{l^2}{ab} \right) - \frac{2}{\pi} \left[\frac{b - \sigma}{b} \frac{l}{a} \sqrt{1 - \frac{(a - \sigma)^2}{l^2}} + \frac{a - \sigma}{a} \frac{l}{b} \sqrt{1 - \frac{(b - \sigma)^2}{l^2}} \right] \\
&\quad + \frac{2}{\pi} \frac{a - \sigma}{a} \frac{b - \sigma}{b} \left(\pi - \arcsin \frac{a - \sigma}{l} - \arcsin \frac{b - \sigma}{l} \right) + \left(\frac{\sigma}{a} + \frac{\sigma}{b} - \frac{\sigma^2}{ab} \right).
\end{aligned} \tag{65}$$

When $\hat{L} < l$, we have $\hat{\phi}_y^* < \hat{\phi}_x^*$. Then,

$$\begin{aligned}
S_{\text{coll}} &= (b - \sigma)A(l, a - \sigma | a - \sigma < l) + (a - \sigma)B(l, b - \sigma | b - \sigma < l) \\
&\quad - AB(l, a - \sigma, b - \sigma | \hat{L} < l) + (\sigma a + \sigma b - \sigma^2) \pi \\
&= ab\pi.
\end{aligned} \tag{66}$$

Thus,

$$P(l, \sigma, a, b) = 1. \tag{67}$$

This result has a similar intuitive interpretation with the case of $L < l$ in the 2D needle version. When a 2D spherocylinder can be fitted in a grid cell, its largest length corresponds to the situation when it aligns with the diagonal line of the grid cell and its two semicircles touch the grid boundaries at two opposite corners. This length is simply \hat{L} . Thus any 2D spherocylinder with a length $l > \hat{L}$ dropped on a grid is certain to intersect with grid lines, leading to $P(l, \sigma, a, b) = 1$.

Summing up the results in Eqs. (61), (63), (65), and (67), we have

$$P(l, \sigma, a, b) = \begin{cases} \frac{2}{\pi} \frac{b - \sigma}{b} \frac{l}{a} + \frac{2}{\pi} \frac{a - \sigma}{a} \frac{l}{b} - \frac{1}{\pi} \frac{l^2}{ab} + \left(\frac{\sigma}{a} + \frac{\sigma}{b} - \frac{\sigma^2}{ab} \right), & \text{if } l \leq b - \sigma; \\ \frac{1}{\pi} \frac{(b - \sigma)^2}{ab} + \frac{2}{\pi} \frac{a - \sigma}{a} \frac{l}{b} \left[1 - \sqrt{1 - \frac{(b - \sigma)^2}{l^2}} \right] \\ + \frac{2}{\pi} \frac{a - \sigma}{a} \frac{b - \sigma}{b} \left(\frac{\pi}{2} - \arcsin \frac{b - \sigma}{l} \right) + \left(\frac{\sigma}{a} + \frac{\sigma}{b} - \frac{\sigma^2}{ab} \right), & \text{if } b - \sigma < l \leq a - \sigma; \\ \frac{1}{\pi} \left(\frac{\hat{L}^2}{ab} + \frac{l^2}{ab} \right) - \frac{2}{\pi} \left[\frac{b - \sigma}{b} \frac{l}{a} \sqrt{1 - \frac{(a - \sigma)^2}{l^2}} + \frac{a - \sigma}{a} \frac{l}{b} \sqrt{1 - \frac{(b - \sigma)^2}{l^2}} \right] \\ + \frac{2}{\pi} \frac{a - \sigma}{a} \frac{b - \sigma}{b} \left(\pi - \arcsin \frac{a - \sigma}{l} - \arcsin \frac{b - \sigma}{l} \right) + \left(\frac{\sigma}{a} + \frac{\sigma}{b} - \frac{\sigma^2}{ab} \right), & \text{if } a - \sigma < l \leq \hat{L}; \\ 1, & \text{if } \hat{L} < l. \end{cases} \tag{68}$$

When $l/a \rightarrow 0$, Eqs.(61) and (63) simplify to the result for the BNP of 2D spherocylinders as

$$P(l, \sigma, \infty, b) = \begin{cases} \frac{2}{\pi} \frac{l}{b} + \frac{\sigma}{b}, & \text{if } l \leq b - \sigma; \\ \frac{2}{\pi} \frac{l}{b} \left[1 - \sqrt{1 - \frac{(b - \sigma)^2}{l^2}} \right] + \frac{2}{\pi} \frac{b - \sigma}{b} \left(\frac{\pi}{2} - \arcsin \frac{b - \sigma}{l} \right) + \frac{\sigma}{b}, & \text{if } b - \sigma < l. \end{cases} \tag{69}$$

We then check the consistence of Eq.(68) at the boundaries of the four cases of $P(l, \sigma, a, b)$, correspondingly S_{coll} . When $l = 0$, in the case of $l \leq b - \sigma$ we have

$$S_{\text{coll}} = (\sigma a + \sigma b - \sigma^2) \pi. \tag{70}$$

Intuitively, a 2D spherocylinder with $l = 0$ reduces to a circle. An intersection between the circle and a grid cell happens when the center of the circle is within a distance of its radius $\sigma/2$ from the four boundaries of the grid cell. We easily have

$$S_{\text{coll}} = [ab - (a - \sigma)(b - \sigma)] \times \pi = (\sigma a + \sigma b - \sigma^2) \pi, \quad (71)$$

which coincides with Eq. (70).

When $l = b - \sigma$, both S_{coll} in the cases of $l \leq b - \sigma$ and $b - \sigma < l \leq a - \sigma$ reduce to

$$S_{\text{coll}} = (b - \sigma)^2 + 2(a - \sigma)(b - \sigma) + (\sigma a + \sigma b - \sigma^2) \pi. \quad (72)$$

When $l = a - \sigma$, both S_{coll} in the cases of $b - \sigma < l \leq a - \sigma$ and $a - \sigma < l \leq \hat{L}$ correspond to

$$\begin{aligned} S_{\text{coll}} &= (b - \sigma)^2 + 2(a - \sigma)^2 \left[1 - \sqrt{1 - \frac{(b - \sigma)^2}{(a - \sigma)^2}} \right] \\ &\quad + 2(a - \sigma)(b - \sigma) \left(\frac{\pi}{2} - \arcsin \frac{b - \sigma}{a - \sigma} \right) + (\sigma a + \sigma b - \sigma^2) \pi. \end{aligned} \quad (73)$$

When $l = \hat{L}$ in the case of $a - \sigma < l \leq \hat{L}$, we have $\cos^2 \hat{\phi}_x^* + \sin^2 \hat{\phi}_y^* = 1$, equivalently $\hat{\phi}_x^* = \hat{\phi}_y^*$. After some calculation we have

$$S_{\text{coll}} = ab\pi, \quad (74)$$

which coincides with the uniform S_{coll} in the case of $\hat{L} < l$ in Eq.(66).

V. THEORY OF BLNP WITH 3D NEEDLES

We follow the analytical framework for the BLNP with 2D needles. We define $S_{\text{all}}^{3\text{D}}$ as the volume of total parameter space of (x_U, y_U, ψ, ϕ) in the case of 3D needles, and $S_{\text{coll}}^{3\text{D}}$ as the volume of proper parameter space of (x_U, y_U, ψ, ϕ) where an intersection happens. The intersection probability is thus

$$P^{3\text{D}}(l, a, b) = \frac{S_{\text{coll}}^{3\text{D}}}{S_{\text{all}}^{3\text{D}}}. \quad (75)$$

For $S_{\text{all}}^{3\text{D}}$, we easily have

$$S_{\text{all}}^{3\text{D}} = ab\pi \frac{\pi}{2}. \quad (76)$$

$S_{\text{coll}}^{3\text{D}}$ can be reformulated as

$$S_{\text{coll}}^{3\text{D}} = S_{\text{coll}}^{3\text{D}}(x) + S_{\text{coll}}^{3\text{D}}(y) - S_{\text{coll}}^{3\text{D}}(x, y), \quad (77)$$

while $S_{\text{coll}}^{3\text{D}}(x)$, $S_{\text{coll}}^{3\text{D}}(y)$, and $S_{\text{coll}}^{3\text{D}}(x, y)$ denote the volume of the parameter space of (x_U, y_U, ψ, ϕ) when an intersection between the projection of a 3D needle and a grid cell happens on the boundaries of the grid cell along the y -axis, the x -axis, and the x - and y -axes at the same time, respectively. Based on Eqs. (3)-(5), and putting an extra $\int_0^{\pi/2} d\psi$ on each term in Eqs.(10)-(12), we have

$$\begin{aligned} S_{\text{coll}}^{3\text{D}}(x) &= b \int_0^{\pi/2} d\psi \int_0^{\pi/2} d\phi \int_0^a \Theta(l \sin \psi \cos \phi - x) dx + b \int_0^{\pi/2} d\psi \int_{\pi/2}^{\pi} d\phi \int_0^a \Theta(-l \sin \psi \cos \phi - x) dx \\ &= b \int_0^{\pi/2} d\psi \int_0^{\pi} d\phi \int_0^a \Theta(|l \sin \psi \cos \phi| - x) dx, \end{aligned} \quad (78)$$

$$S_{\text{coll}}^{3\text{D}}(y) = a \int_0^{\pi/2} d\psi \int_0^{\pi} d\phi \int_0^b \Theta(l \sin \psi \sin \phi - y) dy, \quad (79)$$

$$\begin{aligned} S_{\text{coll}}^{3\text{D}}(x, y) &= \int_0^{\pi/2} d\psi \int_0^{\pi/2} d\phi \int_0^a \Theta(l \sin \psi \cos \phi - x) dx \int_0^b \Theta(l \sin \psi \sin \phi - y) dy \\ &\quad + \int_0^{\pi/2} d\psi \int_{\pi/2}^{\pi} d\phi \int_0^a \Theta(-l \sin \psi \cos \phi - x) dx \int_0^b \Theta(l \sin \psi \sin \phi - y) dy \\ &= \int_0^{\pi/2} d\psi \int_0^{\pi} d\phi \int_0^a \Theta(|l \sin \psi \cos \phi| - x) dx \int_0^b \Theta(l \sin \psi \sin \phi - y) dy. \end{aligned} \quad (80)$$

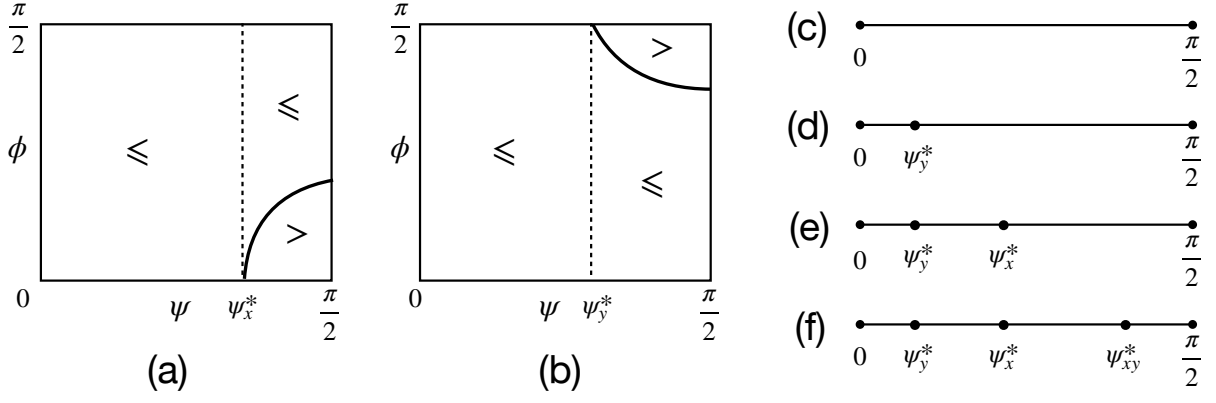


FIG. 3. Schematic diagrams of calculation in the BLNP with 3D needles. (a) The dashed and solid lines correspond to $\psi = \psi_x^*$ and $\phi = \phi_x^*(\psi)$, respectively. The notions \leq and $>$ within diagrams respectively denotes the regions of parameters (ψ, ϕ) when $l \sin \psi \cos \phi \leq a$ and $l \sin \psi \cos \phi > a$ hold. (b) The dashed and solid lines show $\psi = \psi_y^*$ and $\phi = \phi_y^*(\psi)$, respectively. The notions \leq and $>$ respectively denote the regions of parameters (ψ, ϕ) where $l \sin \psi \sin \phi \leq b$ and $l \sin \psi \sin \phi > b$ hold. (c)-(f) Regions of $\psi \in [0, \pi/2]$ when Eqs.(83) is calculated are shown in the cases of $l \leq b$, $b < l \leq a$, $a < l \leq L$, and $L < l$, respectively.

To compute the above equations, we define integrals like Eqs.(16)-(18) as

$$A^{3D}(l, a) \equiv \int_0^{\pi/2} d\psi \int_0^{\pi} d\phi \int_0^a \Theta(|l \sin \psi \cos \phi| - x) dx, \quad (81)$$

$$B^{3D}(l, b) \equiv \int_0^{\pi/2} d\psi \int_0^{\pi} d\phi \int_0^b \Theta(l \sin \psi \sin \phi - y) dy, \quad (82)$$

$$AB^{3D}(l, a, b) \equiv \int_0^{\pi/2} d\psi \int_0^{\pi} d\phi \int_0^a \Theta(|l \sin \psi \cos \phi| - x) dx \int_0^b \Theta(l \sin \psi \sin \phi - y) dy. \quad (83)$$

Thus we reformulate S_{coll}^{3D} as

$$S_{\text{coll}}^{3D} = bA^{3D}(l, a) + aB^{3D}(l, b) - AB^{3D}(l, a, b). \quad (84)$$

We first calculate $A(l, a)$ and $B(l, b)$. We write $A^{3D}(l, a)$ when $l \leq a$ and $a < l$ as $A^{3D}(l, a|l \leq a)$ and $A^{3D}(l, a|a < l)$, respectively. When $l \leq a$, $|l \sin \psi \cos \phi| \leq a$ always holds for any $\psi \in [0, \pi/2]$ and $\phi \in [0, \pi)$. We have

$$\begin{aligned} A^{3D}(l, a|l \leq a) &= \int_0^{\pi/2} d\psi \int_0^{\pi} d\phi \cdot l \sin \psi \cos \phi + \int_0^{\pi/2} d\psi \int_{\pi/2}^{\pi} d\phi \cdot (-l \sin \psi \cos \phi) \\ &= 2l, \end{aligned} \quad (85)$$

When $a < l$, the picture is slightly more complicated. We first define

$$\psi_x^* = \arcsin \frac{a}{l}, \quad (86)$$

$$\phi_x^*(\psi) = \arccos \frac{a}{l \sin \psi}. \quad (87)$$

We can see that, when $\psi \leq \psi_x^*$, we have $l \sin \psi \cos \phi \leq a$ satisfied for any $\phi \in [0, \pi/2]$. Yet when $\psi > \psi_x^*$, two situations happen depending on the value of ϕ : when $\phi \in [\phi_x^*(\psi), \pi/2]$, $l \sin \psi \cos \phi \leq a$ still holds; yet when $\phi \in [0, \phi_x^*(\psi))$, $l \sin \psi \cos \phi > a$ holds instead. A simple schematics is in Fig.3 (a). Later we simply write $\phi_x^*(\psi)$ as ϕ_x^* for short in

this section. We have

$$\begin{aligned}
A^{3D}(l, a|a < l) &= \int_0^{\psi_x^*} d\psi \int_0^{\frac{\pi}{2}} d\phi \cdot l \sin \psi \cos \phi + \int_0^{\psi_x^*} d\psi \int_{\frac{\pi}{2}}^{\pi} d\phi \cdot (-l \sin \psi \cos \phi) \\
&+ \int_{\psi_x^*}^{\frac{\pi}{2}} d\psi \int_0^{\phi_x^*} d\phi \cdot a + \int_{\psi_x^*}^{\frac{\pi}{2}} d\psi \int_{\phi_x^*}^{\frac{\pi}{2}} d\phi \cdot l \sin \psi \cos \phi \\
&+ \int_{\psi_x^*}^{\frac{\pi}{2}} d\psi \int_{\frac{\pi}{2}}^{\pi - \phi_x^*} d\phi \cdot (-l \sin \psi \cos \phi) + \int_{\psi_x^*}^{\frac{\pi}{2}} d\psi \int_{\pi - \phi_x^*}^{\pi} d\phi \cdot a \\
&= 2l - 2l \int_{\psi_x^*}^{\frac{\pi}{2}} d\psi \sqrt{\sin^2 \psi - \frac{a^2}{l^2}} + 2a \int_{\psi_x^*}^{\frac{\pi}{2}} d\psi \left(\frac{\pi}{2} - \arcsin \frac{a}{l \sin \psi} \right) \\
&= 2l - 2lF\left(\psi_x^*, \frac{\pi}{2}, \frac{a}{l}\right) + 2aG\left(\psi_x^*, \frac{\pi}{2}, \frac{a}{l}\right), \tag{88}
\end{aligned}$$

in whose last step we define two integrals respectively as

$$F(a, b, t) \equiv \int_a^b d\psi \sqrt{\sin^2 \psi - t^2}, \tag{89}$$

$$G(a, b, t) \equiv \int_a^b d\psi \left(\frac{\pi}{2} - \arcsin \frac{t}{\sin \psi} \right). \tag{90}$$

These two integrals can be calculated with standard numerical integration methods [17].

We then write $B^{3D}(l, b)$ when $l \leq b$ and $b < l$ as $B^{3D}(l, b|l \leq b)$ and $B^{3D}(l, b|b < l)$, respectively. When $l \leq b$, $l \sin \psi \sin \phi \leq b$ always hold for any $\psi \in [0, \pi/2]$ and $\phi \in [0, \pi)$. We have

$$\begin{aligned}
B^{3D}(l, b|l \leq b) &= \int_0^{\frac{\pi}{2}} d\psi \int_0^{\pi} d\phi \cdot l \sin \psi \sin \phi \\
&= 2l. \tag{91}
\end{aligned}$$

When $b < l$, as in the case of $a < l$ for $A^{3D}(l, a)$, we first define

$$\psi_y^* = \arcsin \frac{b}{l}, \tag{92}$$

$$\phi_y^*(\psi) = \arcsin \frac{b}{l \sin \psi}. \tag{93}$$

We can find that, when $\psi \leq \psi_y^*$, $l \sin \psi \sin \phi \leq b$ is satisfied for any $\phi \in [0, \pi/2]$. Yet when $\psi > \psi_y^*$, two situations happen depending on the value of ϕ : when $\phi \in [0, \phi_y^*(\psi)]$, $l \sin \psi \sin \phi \leq b$ still holds; yet when $\phi \in (\phi_y^*(\psi), \pi/2]$, $l \sin \psi \sin \phi > b$ holds instead. A simple schematics is in Fig.3 (b). Later we simply write $\phi_y^*(\psi)$ as ϕ_y^* for short in this section. We have

$$\begin{aligned}
B^{3D}(l, b|b < l) &= \int_0^{\psi_y^*} d\psi \int_0^{\pi} d\phi \cdot l \sin \psi \sin \phi \\
&+ \int_{\psi_y^*}^{\frac{\pi}{2}} d\psi \int_0^{\phi_y^*} d\phi \cdot l \sin \psi \sin \phi + \int_{\psi_y^*}^{\frac{\pi}{2}} d\psi \int_{\phi_y^*}^{\pi - \phi_y^*} d\phi \cdot b + \int_{\psi_y^*}^{\frac{\pi}{2}} d\psi \int_{\pi - \phi_y^*}^{\pi} d\phi \cdot l \sin \psi \sin \phi \\
&= 2l - 2l \int_{\psi_y^*}^{\frac{\pi}{2}} d\psi \sqrt{\sin^2 \psi - \frac{b^2}{l^2}} + 2b \int_{\psi_y^*}^{\frac{\pi}{2}} d\psi \left(\frac{\pi}{2} - \arcsin \frac{b}{l \sin \psi} \right) \\
&= 2l - 2lF\left(\psi_y^*, \frac{\pi}{2}, \frac{b}{l}\right) + 2bG\left(\psi_y^*, \frac{\pi}{2}, \frac{b}{l}\right). \tag{94}
\end{aligned}$$

To further calculate $AB^{3D}(l, a, b)$ and finally $P^{3D}(l, a, b)$, we consider the following four cases.

A. The case of $l \leq b$

Here the range $\psi \in [0, \pi/2]$ represents a simple case in $AB(l, a, b)$, in which $|l \sin \psi \cos \phi| \leq a$ and $l \sin \psi \sin \phi \leq b$ both hold for any $\phi \in [0, \pi)$. See Fig.3(c) for a schematics. We write $AB^{3D}(l, a, b)$ when $l \leq b$ as $AB^{3D}(l, a, b|l \leq b)$.

We have

$$\begin{aligned} AB^{3D}(l, a, b|l \leq b) &= \int_0^{\frac{\pi}{2}} d\psi \int_0^{\frac{\pi}{2}} d\phi \cdot l \sin \psi \cos \phi \cdot l \sin \psi \sin \phi + \int_0^{\frac{\pi}{2}} d\psi \int_{\frac{\pi}{2}}^{\pi} d\phi \cdot (-l \sin \psi \cos \phi) \cdot l \sin \psi \sin \phi \\ &= S^{(1)}\left(0, \frac{\pi}{2}\right). \end{aligned} \quad (95)$$

In the above equations, we define and calculate a summation as

$$\begin{aligned} S^{(1)}(0, \psi^*) &\equiv \int_0^{\psi^*} d\psi \int_0^{\frac{\pi}{2}} d\phi \cdot l \sin \psi \cos \phi \cdot l \sin \psi \sin \phi + \int_0^{\psi^*} d\psi \int_{\frac{\pi}{2}}^{\pi} d\phi \cdot (-l \sin \psi \cos \phi) \cdot l \sin \psi \sin \phi \\ &= \frac{l^2}{2} (\psi^* - \sin \psi^* \cos \psi^*). \end{aligned} \quad (96)$$

Thus we have

$$S^{(1)}\left(0, \frac{\pi}{2}\right) = \frac{\pi}{4} l^2, \quad (97)$$

$$S^{(1)}(0, \psi_y^*) = \frac{l^2}{2} \psi_y^* - \frac{lb}{2} \cos \psi_y^*. \quad (98)$$

With Eq.(84) we have

$$\begin{aligned} S_{\text{coll}}^{3D} &= bA^{3D}(l, a|l \leq a) + aB^{3D}(l, b|l \leq b) - AB^{3D}(l, a, b|l \leq b) \\ &= 2lb + 2la - \frac{\pi}{4} l^2. \end{aligned} \quad (99)$$

Then,

$$P^{3D}(l, a, b) = \frac{4}{\pi^2} \left(\frac{l}{a} + \frac{l}{b} \right) - \frac{1}{2\pi} \frac{l^2}{ab}. \quad (100)$$

B. The case of $b < l \leq a$

Here we consider the integral on ψ in $AB(l, a, b)$ in two ranges of $[0, \psi_y^*]$ and $(\psi_y^*, \pi/2]$ in a separate way. See Fig.3 (d) for a schematics. We write $AB^{3D}(l, a, b)$ when $b < l \leq a$ as $AB^{3D}(l, a, b|b < l \leq a)$. We have

$$\begin{aligned} &AB^{3D}(l, a, b|b < l \leq a) \\ &= \int_0^{\psi_y^*} d\psi \int_0^{\frac{\pi}{2}} d\phi \cdot l \sin \psi \cos \phi \cdot l \sin \psi \sin \phi + \int_0^{\psi_y^*} d\psi \int_{\frac{\pi}{2}}^{\pi} d\phi \cdot (-l \sin \psi \cos \phi) \cdot l \sin \psi \sin \phi \\ &+ \int_{\psi_y^*}^{\frac{\pi}{2}} d\psi \int_0^{\phi_y^*} d\phi \cdot l \sin \psi \cos \phi \cdot l \sin \psi \sin \phi + \int_{\psi_y^*}^{\frac{\pi}{2}} d\psi \int_{\phi_y^*}^{\frac{\pi}{2}} d\phi \cdot l \sin \psi \cos \phi \cdot b \\ &+ \int_{\psi_y^*}^{\frac{\pi}{2}} d\psi \int_{\frac{\pi}{2}}^{\pi - \phi_y^*} d\phi \cdot (-l \sin \psi \cos \phi) \cdot b + \int_{\psi_y^*}^{\frac{\pi}{2}} d\psi \int_{\pi - \phi_y^*}^{\pi} d\phi \cdot (-l \sin \psi \cos \phi) \cdot l \sin \psi \sin \phi \\ &= S^{(1)}(0, \psi_y^*) + S^{(2)}\left(\psi_y^*, \frac{\pi}{2}\right). \end{aligned} \quad (101)$$

In the above equations, we define and calculate a summation as

$$\begin{aligned} S^{(2)}(\psi_y^*, \psi^*) &\equiv \int_{\psi_y^*}^{\psi^*} d\psi \int_0^{\phi_y^*} d\phi \cdot l \sin \psi \cos \phi \cdot l \sin \psi \sin \phi + \int_{\psi_y^*}^{\psi^*} d\psi \int_{\phi_y^*}^{\frac{\pi}{2}} d\phi \cdot l \sin \psi \cos \phi \cdot b \\ &+ \int_{\psi_y^*}^{\psi^*} d\psi \int_{\frac{\pi}{2}}^{\pi - \phi_y^*} d\phi \cdot (-l \sin \psi \cos \phi) \cdot b + \int_{\psi_y^*}^{\psi^*} d\psi \int_{\pi - \phi_y^*}^{\pi} d\phi \cdot (-l \sin \psi \cos \phi) \cdot l \sin \psi \sin \phi \\ &= 2lb(\cos \psi_y^* - \cos \psi^*) - b^2(\psi^* - \psi_y^*). \end{aligned} \quad (102)$$

Thus we have

$$S^{(2)}\left(\psi_y^*, \frac{\pi}{2}\right) = 2lb \cos \psi_y^* - b^2 \left(\frac{\pi}{2} - \psi_y^*\right), \quad (103)$$

$$S^{(2)}\left(\psi_y^*, \psi_x^*\right) = 2lb(\cos \psi_y^* - \cos \psi_x^*) - b^2(\psi_x^* - \psi_y^*). \quad (104)$$

Then,

$$AB^{3D}(l, a, b|b < l \leq a) = \frac{l^2}{2}\psi_y^* + \frac{3}{2}lb \cos \psi_y^* - b^2 \left(\frac{\pi}{2} - \psi_y^*\right). \quad (105)$$

We have

$$\begin{aligned} S_{\text{coll}}^{3D} &= bA^{3D}(l, a|l \leq a) + aB^{3D}(l, b|b < l) - AB^{3D}(l, a, b|b < l \leq a) \\ &= 2lb + \left[2la - 2laF\left(\psi_y^*, \frac{\pi}{2}, \frac{b}{l}\right) + 2abG\left(\psi_y^*, \frac{\pi}{2}, \frac{b}{l}\right) \right] \\ &\quad - \left[\frac{l^2}{2}\psi_y^* + \frac{3}{2}lb \cos \psi_y^* - b^2 \left(\frac{\pi}{2} - \psi_y^*\right) \right] \\ &= 2lb + \left[2la - 2laF\left(\arcsin \frac{b}{l}, \frac{\pi}{2}, \frac{b}{l}\right) + 2abG\left(\arcsin \frac{b}{l}, \frac{\pi}{2}, \frac{b}{l}\right) \right] \\ &\quad - \left[\frac{l^2}{2} \arcsin \frac{b}{l} + \frac{3}{2}lb \sqrt{1 - \frac{b^2}{l^2}} - b^2 \left(\frac{\pi}{2} - \arcsin \frac{b}{l}\right) \right]. \end{aligned} \quad (106)$$

Then,

$$\begin{aligned} P^{3D}(l, a, b) &= \frac{4}{\pi^2} \frac{l}{a} + \left[\frac{4}{\pi^2} \frac{l}{b} - \frac{4}{\pi^2} \frac{l}{b} F\left(\arcsin \frac{b}{l}, \frac{\pi}{2}, \frac{b}{l}\right) + \frac{4}{\pi^2} G\left(\arcsin \frac{b}{l}, \frac{\pi}{2}, \frac{b}{l}\right) \right] \\ &\quad - \left[\frac{1}{\pi^2} \frac{l^2}{ab} \arcsin \frac{b}{l} + \frac{3}{\pi^2} \frac{l}{a} \sqrt{1 - \frac{b^2}{l^2}} - \frac{2}{\pi^2} \frac{b}{a} \left(\frac{\pi}{2} - \arcsin \frac{b}{l}\right) \right]. \end{aligned} \quad (107)$$

C. The cases in $a < l$

We consider two subcases as $a < l \leq L$ and $L < l$. When $a < l \leq L$, we calculate the integral on ψ in $AB(l, a, b)$ in three ranges of $[0, \psi_y^*]$, $(\psi_y^*, \psi_x^*]$, and $(\psi_x^*, \pi/2]$ in a separate way. See Fig.3 (e) for a schematics. We write $AB^{3D}(l, a, b)$ when $a < l \leq L$ as $AB^{3D}(l, a, b|a < l \leq L)$. We have

$$\begin{aligned} &AB^{3D}(l, a, b|a < l \leq L) \\ &= \int_0^{\psi_y^*} d\psi \int_0^{\frac{\pi}{2}} d\phi \cdot l \sin \psi \cos \phi \cdot l \sin \psi \sin \phi + \int_0^{\psi_y^*} d\psi \int_{\frac{\pi}{2}}^{\pi} d\phi \cdot (-l \sin \psi \cos \phi) \cdot l \sin \psi \sin \phi \\ &\quad + \int_{\psi_y^*}^{\psi_x^*} d\psi \int_0^{\phi_y^*} d\phi \cdot l \sin \psi \cos \phi \cdot l \sin \psi \sin \phi + \int_{\psi_y^*}^{\psi_x^*} d\psi \int_{\phi_y^*}^{\frac{\pi}{2}} d\phi \cdot l \sin \psi \cos \phi \cdot b \\ &\quad + \int_{\psi_y^*}^{\psi_x^*} d\psi \int_{\frac{\pi}{2}}^{\pi - \phi_y^*} d\phi \cdot (-l \sin \psi \cos \phi) \cdot b + \int_{\psi_y^*}^{\psi_x^*} d\psi \int_{\pi - \phi_y^*}^{\pi} d\phi \cdot (-l \sin \psi \cos \phi) \cdot l \sin \psi \sin \phi \\ &\quad + \int_{\psi_x^*}^{\frac{\pi}{2}} d\psi \int_0^{\phi_x^*} d\phi \cdot a \cdot l \sin \psi \sin \phi + \int_{\psi_x^*}^{\frac{\pi}{2}} d\psi \int_{\phi_x^*}^{\phi_y^*} d\phi \cdot l \sin \psi \cos \phi \cdot l \sin \psi \sin \phi \\ &\quad + \int_{\psi_x^*}^{\frac{\pi}{2}} d\psi \int_{\phi_y^*}^{\frac{\pi}{2}} d\phi \cdot l \sin \psi \cos \phi \cdot b \\ &\quad + \int_{\psi_x^*}^{\frac{\pi}{2}} d\psi \int_{\frac{\pi}{2}}^{\pi - \phi_y^*} d\phi \cdot (-l \sin \psi \cos \phi) \cdot b + \int_{\psi_x^*}^{\frac{\pi}{2}} d\psi \int_{\pi - \phi_y^*}^{\pi - \phi_x^*} d\phi \cdot (-l \sin \psi \cos \phi) \cdot l \sin \psi \sin \phi \\ &\quad + \int_{\psi_x^*}^{\frac{\pi}{2}} d\psi \int_{\pi - \phi_x^*}^{\pi} d\phi \cdot a \cdot l \sin \psi \sin \phi \\ &= S^{(1)}(0, \psi_y^*) + S^{(2)}(\psi_y^*, \psi_x^*) + S^{(3)}\left(\psi_x^*, \frac{\pi}{2}\right). \end{aligned} \quad (108)$$

In the above equations, we define and calculate a summation as

$$\begin{aligned}
S^{(3)}(\psi_x^*, \psi^*) &\equiv \int_{\psi_x^*}^{\psi^*} d\psi \int_0^{\phi_x^*} d\phi \cdot a \cdot l \sin \psi \sin \phi + \int_{\psi_x^*}^{\psi^*} d\psi \int_{\phi_x^*}^{\phi_y^*} d\phi \cdot l \sin \psi \cos \phi \cdot l \sin \psi \sin \phi \\
&+ \int_{\psi_x^*}^{\psi^*} d\psi \int_{\phi_y^*}^{\frac{\pi}{2}} d\phi \cdot l \sin \psi \cos \phi \cdot b \\
&+ \int_{\psi_x^*}^{\psi^*} d\psi \int_{\frac{\pi}{2}}^{\pi - \phi_y^*} d\phi \cdot (-l \sin \psi \cos \phi) \cdot b + \int_{\psi_x^*}^{\psi^*} d\psi \int_{\pi - \phi_x^*}^{\pi - \phi_y^*} d\phi \cdot (-l \sin \psi \cos \phi) \cdot l \sin \psi \sin \phi \\
&+ \int_{\psi_x^*}^{\psi^*} d\psi \int_{\pi - \phi_x^*}^{\pi} d\phi \cdot a \cdot l \sin \psi \sin \phi \\
&= 2la(\cos \psi_x^* - \cos \psi^*) - a^2(\psi^* - \psi_x^*) + 2lb(\cos \psi_x^* - \cos \psi^*) - b^2(\psi^* - \psi_x^*) \\
&- \left[\left(\frac{l^2}{2} \psi^* - \frac{l^2}{2} \sin \psi^* \cos \psi^* \right) - \left(\frac{l^2}{2} \psi_x^* - \frac{l^2}{2} \sin \psi_x^* \cos \psi_x^* \right) \right]. \tag{109}
\end{aligned}$$

Thus we have

$$\begin{aligned}
S^{(3)}\left(\psi_x^*, \frac{\pi}{2}\right) &= 2la \cos \psi_x^* - a^2 \left(\frac{\pi}{2} - \psi_x^* \right) + 2lb \cos \psi_x^* - b^2 \left(\frac{\pi}{2} - \psi_x^* \right) \\
&- \left[\frac{\pi}{4} l^2 - \left(\frac{l^2}{2} \psi_x^* - \frac{la}{2} \cos \psi_x^* \right) \right], \tag{110}
\end{aligned}$$

$$\begin{aligned}
S^{(3)}(\psi_x^*, \psi_{xy}^*) &= 2la(\cos \psi_x^* - \cos \psi_{xy}^*) - a^2(\psi_{xy}^* - \psi_x^*) + 2lb(\cos \psi_x^* - \cos \psi_{xy}^*) - b^2(\psi_{xy}^* - \psi_x^*) \\
&- \left[\left(\frac{l^2}{2} \psi_{xy}^* - \frac{lL}{2} \cos \psi_{xy}^* \right) - \left(\frac{l^2}{2} \psi_x^* - \frac{la}{2} \cos \psi_x^* \right) \right], \tag{111}
\end{aligned}$$

in which we define

$$\psi_{xy}^* = \arcsin \frac{L}{l}. \tag{112}$$

Then,

$$AB^{3D}(l, a, b|a < l \leq L) = \left[\frac{l^2}{2} \psi_x^* + \frac{3}{2} la \cos \psi_x^* - a^2 \left(\frac{\pi}{2} - \psi_x^* \right) \right] + \left[\frac{l^2}{2} \psi_y^* + \frac{3}{2} lb \cos \psi_y^* - b^2 \left(\frac{\pi}{2} - \psi_y^* \right) \right] - \frac{\pi}{4} l^2 \tag{113}$$

We have

$$\begin{aligned}
S_{\text{coll}}^{3D} &= bA^{3D}(l, a|a < l) + aB^{3D}(l, b|b < l) - AB^{3D}(l, a, b|a < l \leq L) \\
&= \left[2lb - 2lbF\left(\psi_x^*, \frac{\pi}{2}, \frac{a}{l}\right) + 2abG\left(\psi_x^*, \frac{\pi}{2}, \frac{a}{l}\right) \right] + \left[2la - 2laF\left(\psi_y^*, \frac{\pi}{2}, \frac{b}{l}\right) + 2abG\left(\psi_y^*, \frac{\pi}{2}, \frac{b}{l}\right) \right] \\
&- \left[\frac{l^2}{2} \psi_x^* + \frac{3}{2} la \cos \psi_x^* - a^2 \left(\frac{\pi}{2} - \psi_x^* \right) \right] - \left[\frac{l^2}{2} \psi_y^* + \frac{3}{2} lb \cos \psi_y^* - b^2 \left(\frac{\pi}{2} - \psi_y^* \right) \right] + \frac{\pi}{4} l^2 \\
&= \left[2lb - 2lbF\left(\arcsin \frac{a}{l}, \frac{\pi}{2}, \frac{a}{l}\right) + 2abG\left(\arcsin \frac{a}{l}, \frac{\pi}{2}, \frac{a}{l}\right) \right] \\
&+ \left[2la - 2laF\left(\arcsin \frac{b}{l}, \frac{\pi}{2}, \frac{b}{l}\right) + 2abG\left(\arcsin \frac{b}{l}, \frac{\pi}{2}, \frac{b}{l}\right) \right] \\
&- \left[\frac{l^2}{2} \arcsin \frac{a}{l} + \frac{3}{2} la \sqrt{1 - \frac{a^2}{l^2}} - a^2 \left(\frac{\pi}{2} - \arcsin \frac{a}{l} \right) \right] \\
&- \left[\frac{l^2}{2} \arcsin \frac{b}{l} + \frac{3}{2} lb \sqrt{1 - \frac{b^2}{l^2}} - b^2 \left(\frac{\pi}{2} - \arcsin \frac{b}{l} \right) \right] + \frac{\pi}{4} l^2. \tag{114}
\end{aligned}$$

Then,

$$\begin{aligned}
P^{3D}(l, a, b) &= \left[\frac{4}{\pi^2} \frac{l}{a} - \frac{4}{\pi^2} \frac{l}{a} F\left(\arcsin \frac{a}{l}, \frac{\pi}{2}, \frac{a}{l}\right) + \frac{4}{\pi^2} G\left(\arcsin \frac{a}{l}, \frac{\pi}{2}, \frac{a}{l}\right) \right] \\
&+ \left[\frac{4}{\pi^2} \frac{l}{b} - \frac{4}{\pi^2} \frac{l}{b} F\left(\arcsin \frac{b}{l}, \frac{\pi}{2}, \frac{b}{l}\right) + \frac{4}{\pi^2} G\left(\arcsin \frac{b}{l}, \frac{\pi}{2}, \frac{b}{l}\right) \right] \\
&- \left[\frac{1}{\pi^2} \frac{l^2}{ab} \arcsin \frac{a}{l} + \frac{3}{\pi^2} \frac{l}{b} \sqrt{1 - \frac{a^2}{l^2}} - \frac{2}{\pi^2} \frac{a}{b} \left(\frac{\pi}{2} - \arcsin \frac{a}{l}\right) \right] \\
&- \left[\frac{1}{\pi^2} \frac{l^2}{ab} \arcsin \frac{b}{l} + \frac{3}{\pi^2} \frac{l}{a} \sqrt{1 - \frac{b^2}{l^2}} - \frac{2}{\pi^2} \frac{b}{a} \left(\frac{\pi}{2} - \arcsin \frac{b}{l}\right) \right] + \frac{1}{2\pi} \frac{l^2}{ab}. \tag{115}
\end{aligned}$$

When $L < l$, we calculate the integral on ψ in $AB(l, a, b)$ in four ranges of $[0, \psi_y^*]$, $(\psi_y^*, \psi_x^*]$, $(\psi_y^*, \psi_{xy}^*]$, and $(\psi_{xy}^*, \pi/2]$ in a separate way. See Fig.3 (f) for a schematics. We write $AB^{3D}(l, a, b)$ when $L < l$ as $AB^{3D}(l, a, b|L < l)$, and have

$$\begin{aligned}
&AB^{3D}(l, a, b|L < l) \\
&= \int_0^{\psi_y^*} d\psi \int_0^{\frac{\pi}{2}} d\phi \cdot l \sin \psi \cos \phi \cdot l \sin \psi \sin \phi + \int_0^{\psi_y^*} d\psi \int_{\frac{\pi}{2}}^{\pi} d\phi \cdot (-l \sin \psi \cos \phi) \cdot l \sin \psi \sin \phi \\
&+ \int_{\psi_y^*}^{\psi_x^*} d\psi \int_0^{\phi_y^*} d\phi \cdot l \sin \psi \cos \phi \cdot l \sin \psi \sin \phi + \int_{\psi_y^*}^{\psi_x^*} d\psi \int_{\phi_y^*}^{\frac{\pi}{2}} d\phi \cdot l \sin \psi \cos \phi \cdot b \\
&+ \int_{\psi_y^*}^{\psi_x^*} d\psi \int_{\frac{\pi}{2}}^{\pi - \phi_y^*} d\phi \cdot (-l \sin \psi \cos \phi) \cdot b + \int_{\psi_y^*}^{\psi_x^*} d\psi \int_{\pi - \phi_y^*}^{\pi} d\phi \cdot (-l \sin \psi \cos \phi) \cdot l \sin \psi \sin \phi \\
&+ \int_{\psi_x^*}^{\psi_{xy}^*} d\psi \int_0^{\phi_x^*} d\phi \cdot a \cdot l \sin \psi \sin \phi + \int_{\psi_x^*}^{\psi_{xy}^*} d\psi \int_{\phi_x^*}^{\phi_y^*} d\phi \cdot l \sin \psi \cos \phi \cdot l \sin \psi \sin \phi \\
&+ \int_{\psi_x^*}^{\psi_{xy}^*} d\psi \int_{\phi_y^*}^{\frac{\pi}{2}} d\phi \cdot l \sin \psi \cos \phi \cdot b \\
&+ \int_{\psi_x^*}^{\psi_{xy}^*} d\psi \int_{\frac{\pi}{2}}^{\pi - \phi_x^*} d\phi \cdot (-l \sin \psi \cos \phi) \cdot b + \int_{\psi_x^*}^{\psi_{xy}^*} d\psi \int_{\pi - \phi_x^*}^{\pi - \phi_y^*} d\phi \cdot (-l \sin \psi \cos \phi) \cdot l \sin \psi \sin \phi \\
&+ \int_{\psi_x^*}^{\psi_{xy}^*} d\psi \int_{\pi - \phi_x^*}^{\pi} d\phi \cdot a \cdot l \sin \psi \sin \phi \\
&+ \int_{\psi_{xy}^*}^{\frac{\pi}{2}} d\psi \int_0^{\phi_y^*} d\phi \cdot a \cdot l \sin \psi \sin \phi + \int_{\psi_{xy}^*}^{\frac{\pi}{2}} d\psi \int_{\phi_y^*}^{\phi_x^*} d\phi \cdot a \cdot b + \int_{\psi_{xy}^*}^{\frac{\pi}{2}} d\psi \int_{\phi_x^*}^{\frac{\pi}{2}} d\phi \cdot l \sin \psi \cos \phi \cdot b \\
&+ \int_{\psi_{xy}^*}^{\frac{\pi}{2}} d\psi \int_{\frac{\pi}{2}}^{\pi - \phi_x^*} d\phi \cdot (-l \sin \psi \cos \phi) \cdot b + \int_{\psi_{xy}^*}^{\frac{\pi}{2}} d\psi \int_{\pi - \phi_x^*}^{\pi - \phi_y^*} d\phi \cdot a \cdot b + \int_{\psi_{xy}^*}^{\frac{\pi}{2}} d\psi \int_{\pi - \phi_y^*}^{\pi} d\phi \cdot a \cdot l \sin \psi \sin \phi \\
&= S^{(1)}(0, \psi_y^*) + S^{(2)}(\psi_y^*, \psi_x^*) + S^{(3)}(\psi_x^*, \psi_{xy}^*) + S^{(4)}\left(\psi_{xy}^*, \frac{\pi}{2}\right). \tag{116}
\end{aligned}$$

In the above equations, we define and calculate a summation as

$$\begin{aligned}
S^{(4)}\left(\psi_{xy}^*, \frac{\pi}{2}\right) &= \int_{\psi_{xy}^*}^{\frac{\pi}{2}} d\psi \int_0^{\phi_y^*} d\phi \cdot a \cdot l \sin \psi \sin \phi + \int_{\psi_{xy}^*}^{\frac{\pi}{2}} d\psi \int_{\phi_y^*}^{\phi_x^*} d\phi \cdot a \cdot b + \int_{\psi_{xy}^*}^{\frac{\pi}{2}} d\psi \int_{\phi_x^*}^{\frac{\pi}{2}} d\phi \cdot l \sin \psi \cos \phi \cdot b \\
&+ \int_{\psi_{xy}^*}^{\frac{\pi}{2}} d\psi \int_{\frac{\pi}{2}}^{\pi - \phi_x^*} d\phi \cdot (-l \sin \psi \cos \phi) \cdot b + \int_{\psi_{xy}^*}^{\frac{\pi}{2}} d\psi \int_{\pi - \phi_x^*}^{\pi - \phi_y^*} d\phi \cdot a \cdot b + \int_{\psi_{xy}^*}^{\frac{\pi}{2}} d\psi \int_{\pi - \phi_y^*}^{\pi} d\phi \cdot a \cdot l \sin \psi \sin \phi \\
&= \left[2lb \cos \psi_{xy}^* - 2lbF\left(\psi_{xy}^*, \frac{\pi}{2}, \frac{a}{l}\right) + 2abG\left(\psi_{xy}^*, \frac{\pi}{2}, \frac{a}{l}\right) \right] \\
&+ \left[2la \cos \psi_{xy}^* - 2laF\left(\psi_{xy}^*, \frac{\pi}{2}, \frac{b}{l}\right) + 2abG\left(\psi_{xy}^*, \frac{\pi}{2}, \frac{b}{l}\right) \right] - ab\pi \left(\frac{\pi}{2} - \psi_{xy}^*\right). \tag{117}
\end{aligned}$$

Thus we have

$$\begin{aligned}
AB^{3D}(l, a, b|L < l) &= \left[-2lbF\left(\psi_{xy}^*, \frac{\pi}{2}, \frac{a}{l}\right) + 2abG\left(\psi_{xy}^*, \frac{\pi}{2}, \frac{a}{l}\right) \right] + \left[-2laF\left(\psi_{xy}^*, \frac{\pi}{2}, \frac{b}{l}\right) + 2abG\left(\psi_{xy}^*, \frac{\pi}{2}, \frac{b}{l}\right) \right] \\
&+ \left[\frac{l^2}{2}\psi_x^* + \frac{3}{2}la \cos \psi_x^* - a^2 \left(\frac{\pi}{2} - \psi_x^*\right) \right] + \left[\frac{l^2}{2}\psi_y^* + \frac{3}{2}lb \cos \psi_y^* - b^2 \left(\frac{\pi}{2} - \psi_y^*\right) \right] \\
&- \left[\frac{l^2}{2}\psi_{xy}^* - \frac{lL}{2} \cos \psi_{xy}^* - L^2 \left(\frac{\pi}{2} - \psi_{xy}^*\right) \right] - ab\pi \left(\frac{\pi}{2} - \psi_{xy}^*\right). \tag{118}
\end{aligned}$$

We have

$$\begin{aligned}
S_{\text{coll}}^{3D} &= bA^{3D}(l, a|a < l) + aB^{3D}(l, b|b < l) - AB^{3D}(l, a, b|L < l) \\
&= \left[2lb - 2lbF\left(\psi_x^*, \psi_{xy}^*, \frac{a}{l}\right) + 2abG\left(\psi_x^*, \psi_{xy}^*, \frac{a}{l}\right) \right] + \left[2la - 2laF\left(\psi_y^*, \psi_{xy}^*, \frac{b}{l}\right) + 2abG\left(\psi_y^*, \psi_{xy}^*, \frac{b}{l}\right) \right] \\
&- \left[\frac{l^2}{2}\psi_x^* + \frac{3}{2}la \cos \psi_x^* - a^2 \left(\frac{\pi}{2} - \psi_x^*\right) \right] - \left[\frac{l^2}{2}\psi_y^* + \frac{3}{2}lb \cos \psi_y^* - b^2 \left(\frac{\pi}{2} - \psi_y^*\right) \right] \\
&+ \left[\frac{l^2}{2}\psi_{xy}^* - \frac{lL}{2} \cos \psi_{xy}^* - L^2 \left(\frac{\pi}{2} - \psi_{xy}^*\right) \right] + ab\pi \left(\frac{\pi}{2} - \psi_{xy}^*\right) \\
&= \left[2lb - 2lbF\left(\arcsin \frac{a}{l}, \arcsin \frac{L}{l}, \frac{a}{l}\right) + 2abG\left(\arcsin \frac{a}{l}, \arcsin \frac{L}{l}, \frac{a}{l}\right) \right] \\
&+ \left[2la - 2laF\left(\arcsin \frac{b}{l}, \arcsin \frac{L}{l}, \frac{b}{l}\right) + 2abG\left(\arcsin \frac{b}{l}, \arcsin \frac{L}{l}, \frac{b}{l}\right) \right] \\
&- \left[\frac{l^2}{2} \arcsin \frac{a}{l} + \frac{3}{2}la \sqrt{1 - \frac{a^2}{l^2}} - a^2 \left(\frac{\pi}{2} - \arcsin \frac{a}{l}\right) \right] \\
&- \left[\frac{l^2}{2} \arcsin \frac{b}{l} + \frac{3}{2}lb \sqrt{1 - \frac{b^2}{l^2}} - b^2 \left(\frac{\pi}{2} - \arcsin \frac{b}{l}\right) \right] \\
&+ \left[\frac{l^2}{2} \arcsin \frac{L}{l} - \frac{lL}{2} \sqrt{1 - \frac{L^2}{l^2}} - L^2 \left(\frac{\pi}{2} - \arcsin \frac{L}{l}\right) \right] + ab\pi \left(\frac{\pi}{2} - \arcsin \frac{L}{l}\right). \tag{119}
\end{aligned}$$

Then,

$$\begin{aligned}
P^{3D}(l, a, b) &= \left[\frac{4}{\pi^2} \frac{l}{a} - \frac{4}{\pi^2} \frac{l}{a} F\left(\arcsin \frac{a}{l}, \arcsin \frac{L}{l}, \frac{a}{l}\right) + \frac{4}{\pi^2} G\left(\arcsin \frac{a}{l}, \arcsin \frac{L}{l}, \frac{a}{l}\right) \right] \\
&+ \left[\frac{4}{\pi^2} \frac{l}{b} - \frac{4}{\pi^2} \frac{l}{b} F\left(\arcsin \frac{b}{l}, \arcsin \frac{L}{l}, \frac{b}{l}\right) + \frac{4}{\pi^2} G\left(\arcsin \frac{b}{l}, \arcsin \frac{L}{l}, \frac{b}{l}\right) \right] \\
&- \left[\frac{1}{\pi^2} \frac{l^2}{ab} \arcsin \frac{a}{l} + \frac{3}{\pi^2} \frac{l}{b} \sqrt{1 - \frac{a^2}{l^2}} - \frac{2}{\pi^2} \frac{a}{b} \left(\frac{\pi}{2} - \arcsin \frac{a}{l}\right) \right] \\
&- \left[\frac{1}{\pi^2} \frac{l^2}{ab} \arcsin \frac{b}{l} + \frac{3}{\pi^2} \frac{l}{a} \sqrt{1 - \frac{b^2}{l^2}} - \frac{2}{\pi^2} \frac{b}{a} \left(\frac{\pi}{2} - \arcsin \frac{b}{l}\right) \right] \\
&+ \left[\frac{1}{\pi^2} \frac{l^2}{ab} \arcsin \frac{L}{l} - \frac{1}{\pi^2} \frac{lL}{ab} \sqrt{1 - \frac{L^2}{l^2}} - \frac{2}{\pi^2} \frac{L^2}{ab} \left(\frac{\pi}{2} - \arcsin \frac{L}{l}\right) \right] + \frac{2}{\pi} \left(\frac{\pi}{2} - \arcsin \frac{L}{l}\right). \tag{120}
\end{aligned}$$

D. Summed results

Summing up the results in Eqs. (100), (107), (115), and (120), we have

$$P^{3D}(l, a, b) = \begin{cases} \left[\frac{4}{\pi^2} \left(\frac{l}{a} + \frac{l}{b} \right) - \frac{1}{2\pi} \frac{l^2}{ab} \right], & \text{if } l \leq b; \\ \left[\frac{4}{\pi^2} \frac{l}{a} + \left[\frac{4}{\pi^2} \frac{l}{b} - \frac{4}{\pi^2} \frac{l}{b} F \left(\arcsin \frac{b}{l}, \frac{\pi}{2}, \frac{b}{l} \right) + \frac{4}{\pi^2} G \left(\arcsin \frac{b}{l}, \frac{\pi}{2}, \frac{b}{l} \right) \right] \right. \\ \quad \left. - \left[\frac{1}{\pi^2} \frac{l^2}{ab} \arcsin \frac{b}{l} + \frac{3}{\pi^2} \frac{l}{a} \sqrt{1 - \frac{b^2}{l^2}} - \frac{2}{\pi^2} \frac{b}{a} \left(\frac{\pi}{2} - \arcsin \frac{b}{l} \right) \right] \right], & \text{if } b < l \leq a; \\ \left[\frac{4}{\pi^2} \frac{l}{a} - \frac{4}{\pi^2} \frac{l}{a} F \left(\arcsin \frac{a}{l}, \frac{\pi}{2}, \frac{a}{l} \right) + \frac{4}{\pi^2} G \left(\arcsin \frac{a}{l}, \frac{\pi}{2}, \frac{a}{l} \right) \right] \\ \quad + \left[\frac{4}{\pi^2} \frac{l}{b} - \frac{4}{\pi^2} \frac{l}{b} F \left(\arcsin \frac{b}{l}, \frac{\pi}{2}, \frac{b}{l} \right) + \frac{4}{\pi^2} G \left(\arcsin \frac{b}{l}, \frac{\pi}{2}, \frac{b}{l} \right) \right] \\ \quad - \left[\frac{1}{\pi^2} \frac{l^2}{ab} \arcsin \frac{a}{l} + \frac{3}{\pi^2} \frac{l}{b} \sqrt{1 - \frac{a^2}{l^2}} - \frac{2}{\pi^2} \frac{a}{b} \left(\frac{\pi}{2} - \arcsin \frac{a}{l} \right) \right] \\ \quad - \left[\frac{1}{\pi^2} \frac{l^2}{ab} \arcsin \frac{b}{l} + \frac{3}{\pi^2} \frac{l}{a} \sqrt{1 - \frac{b^2}{l^2}} - \frac{2}{\pi^2} \frac{b}{a} \left(\frac{\pi}{2} - \arcsin \frac{b}{l} \right) \right] \\ \quad + \frac{1}{2\pi} \frac{l^2}{ab}, & \text{if } a < l \leq L; \\ \left[\frac{4}{\pi^2} \frac{l}{a} - \frac{4}{\pi^2} \frac{l}{a} F \left(\arcsin \frac{L}{l}, \arcsin \frac{L}{l}, \frac{a}{l} \right) + \frac{4}{\pi^2} G \left(\arcsin \frac{L}{l}, \arcsin \frac{L}{l}, \frac{a}{l} \right) \right] \\ \quad + \left[\frac{4}{\pi^2} \frac{l}{b} - \frac{4}{\pi^2} \frac{l}{b} F \left(\arcsin \frac{L}{l}, \arcsin \frac{L}{l}, \frac{b}{l} \right) + \frac{4}{\pi^2} G \left(\arcsin \frac{L}{l}, \arcsin \frac{L}{l}, \frac{b}{l} \right) \right] \\ \quad - \left[\frac{1}{\pi^2} \frac{l^2}{ab} \arcsin \frac{a}{l} + \frac{3}{\pi^2} \frac{l}{b} \sqrt{1 - \frac{a^2}{l^2}} - \frac{2}{\pi^2} \frac{a}{b} \left(\frac{\pi}{2} - \arcsin \frac{a}{l} \right) \right] \\ \quad - \left[\frac{1}{\pi^2} \frac{l^2}{ab} \arcsin \frac{b}{l} + \frac{3}{\pi^2} \frac{l}{a} \sqrt{1 - \frac{b^2}{l^2}} - \frac{2}{\pi^2} \frac{b}{a} \left(\frac{\pi}{2} - \arcsin \frac{b}{l} \right) \right] \\ \quad + \left[\frac{1}{\pi^2} \frac{l^2}{ab} \arcsin \frac{L}{l} - \frac{1}{\pi^2} \frac{LL}{ab} \sqrt{1 - \frac{L^2}{l^2}} - \frac{2}{\pi^2} \frac{L^2}{ab} \left(\frac{\pi}{2} - \arcsin \frac{L}{l} \right) \right] + \frac{2}{\pi} \left(\frac{\pi}{2} - \arcsin \frac{L}{l} \right), & \text{if } L < l. \end{cases} \quad (121)$$

When $l/a \rightarrow 0$, Eqs.(100) and (107) simplify to the result for the BNP with 3D needles as

$$P^{3D}(l, \infty, b) = \begin{cases} \frac{4}{\pi^2} \frac{l}{b}, & \text{if } l \leq b; \\ \frac{4}{\pi^2} \frac{l}{b} - \frac{4}{\pi^2} \frac{l}{b} F \left(\arcsin \frac{b}{l}, \frac{\pi}{2}, \frac{b}{l} \right) + \frac{4}{\pi^2} G \left(\arcsin \frac{b}{l}, \frac{\pi}{2}, \frac{b}{l} \right), & \text{if } b < l. \end{cases} \quad (122)$$

We then check the consistency of Eq.(121) at the boundaries of the four cases of $P^{3D}(l, a, b)$, equivalently S_{coll}^{3D} . When $l = 0$, in the case of $l \leq b$, we have $P^{3D}(0, a, b) = 0$, which is intuitively correct.

When $l = b$, both the cases of $l \leq b$ and $b < l \leq a$ lead to

$$S_{\text{coll}}^{3D} = \left(2 - \frac{\pi}{4} \right) b^2 + 2ab. \quad (123)$$

When $l = a$, both the cases of $b < l \leq a$ and $a < l \leq L$ correspond to

$$S_{\text{coll}}^{3D} = 2ab + \left[2a^2 - 2a^2 F \left(\arcsin \frac{b}{a}, \frac{\pi}{2}, \frac{b}{a} \right) + 2abG \left(\arcsin \frac{b}{a}, \frac{\pi}{2}, \frac{b}{a} \right) \right] \\ - \left[\frac{a^2}{2} \arcsin \frac{b}{a} + \frac{3}{2} ab \sqrt{1 - \frac{b^2}{a^2}} - b^2 \left(\frac{\pi}{2} - \arcsin \frac{b}{a} \right) \right]. \quad (124)$$

When $l = L$, both the cases of $a < l \leq L$ and $L < l$ result in

$$S_{\text{coll}}^{3D} = \left[2bL - 2bLF \left(\arcsin \frac{a}{L}, \frac{\pi}{2}, \frac{a}{L} \right) + 2abG \left(\arcsin \frac{a}{L}, \frac{\pi}{2}, \frac{a}{L} \right) \right] \\ + \left[2aL - 2aLF \left(\arcsin \frac{b}{L}, \frac{\pi}{2}, \frac{b}{L} \right) + 2abG \left(\arcsin \frac{b}{L}, \frac{\pi}{2}, \frac{b}{L} \right) \right] \\ - \left[3ab - a^2 \left(\frac{\pi}{2} - \arcsin \frac{a}{L} \right) - b^2 \left(\frac{\pi}{2} - \arcsin \frac{b}{L} \right) \right]. \quad (125)$$

Finally we consider the case of $l \rightarrow \infty$. For a general integral $H(a, b, t) \equiv \int_a^b d\psi h(\psi, t)$, if $a, b \rightarrow 0$ and both $h(a, t)$ and $h(b, t)$ are well-defined and finite, we have

$$H(a, b, t) \sim \frac{1}{2} (b - a) [h(a, t) + h(b, t)], \quad (126)$$

based on the Trapezoidal rule in numerical integration methods [17]. Thus we have

$$\begin{aligned} lbF\left(\arcsin \frac{a}{l}, \arcsin \frac{L}{l}, \frac{a}{l}\right) &\sim lb \cdot \frac{1}{2} \left(\arcsin \frac{L}{l} - \arcsin \frac{a}{l}\right) \left[\sqrt{\frac{L^2}{l^2} - \frac{a^2}{l^2}} + \sqrt{\frac{a^2}{l^2} - \frac{a^2}{l^2}}\right] \\ &= \frac{1}{2}b^2 \left(\arcsin \frac{L}{l} - \arcsin \frac{a}{l}\right) \rightarrow 0, \end{aligned} \quad (127)$$

$$laF\left(\arcsin \frac{b}{l}, \arcsin \frac{L}{l}, \frac{b}{l}\right) \sim \frac{1}{2}a^2 \left(\arcsin \frac{L}{l} - \arcsin \frac{b}{l}\right) \rightarrow 0. \quad (128)$$

We further have

$$\begin{aligned} G\left(\arcsin \frac{a}{l}, \arcsin \frac{L}{l}, \frac{a}{l}\right) &\sim \frac{1}{2} \left(\arcsin \frac{L}{l} - \arcsin \frac{a}{l}\right) \left[\left(\frac{\pi}{2} - \arcsin \frac{a/l}{L/l}\right) + \left(\frac{\pi}{2} - \arcsin \frac{a/l}{a/l}\right)\right] \\ &= \frac{1}{2} \left(\arcsin \frac{L}{l} - \arcsin \frac{a}{l}\right) \left(\frac{\pi}{2} - \arcsin \frac{a}{L}\right) \rightarrow 0, \end{aligned} \quad (129)$$

$$G\left(\arcsin \frac{b}{l}, \arcsin \frac{L}{l}, \frac{b}{l}\right) \sim \frac{1}{2} \left(\arcsin \frac{L}{l} - \arcsin \frac{b}{l}\right) \left(\frac{\pi}{2} - \arcsin \frac{b}{L}\right) \rightarrow 0. \quad (130)$$

Summing up Eqs.(127)-(130), Eq.(119) reduces to

$$\begin{aligned} S_{\text{coll}}^{3\text{D}} &= [2lb - 2 \cdot 0 + 2ab \cdot 0] + [2la - 2 \cdot 0 + 2ab \cdot 0] \\ &\quad - \left[\frac{l^2}{2} \cdot \frac{a}{l} + \frac{3}{2}la \cdot \sqrt{1-0} - a^2 \cdot \left(\frac{\pi}{2} - 0\right)\right] - \left[\frac{l^2}{2} \cdot \frac{b}{l} + \frac{3}{2}lb \cdot \sqrt{1-0} - b^2 \cdot \left(\frac{\pi}{2} - 0\right)\right] \\ &\quad + \left[\frac{l^2}{2} \cdot \frac{L}{l} - \frac{lL}{2} \cdot \sqrt{1-0} - L^2 \cdot \left(\frac{\pi}{2} - 0\right)\right] + ab\pi \cdot \left(\frac{\pi}{2} - 0\right) \\ &= ab \frac{\pi^2}{2}. \end{aligned} \quad (131)$$

Correspondingly, $P^{3\text{D}}(\infty, a, b) = 1$. This is intuitively understandable. The projection of a finite long needle onto a 2D plane eludes the boundaries of a grid cell with a non-vanishing probability, since the orientation ψ always has a finite, even narrow, range to trigger an intersection. Only an infinitely long needle is sure to intersect with the grid.

VI. THEORY OF BLNP WITH 3D SPHEROCYLINDERS

We follow the framework for the BLNP with 3D needles, and calculate the intersection probability for the BLNP with 3D spherocylinders here as

$$P^{3\text{D}}(l, \sigma, a, b) = \frac{S_{\text{coll}}^{3\text{D}}}{S_{\text{all}}^{3\text{D}}}. \quad (132)$$

$S_{\text{coll}}^{3\text{D}}$ can be further reformulated as Eq.(77). $S_{\text{coll}}^{3\text{D}}(x)$, $S_{\text{coll}}^{3\text{D}}(y)$, and $S_{\text{coll}}^{3\text{D}}(x, y)$ denote the volume of the parameter space of (x_U, y_U, ψ, ϕ) when an intersection between the projection of a 3D spherocylinder and a grid cell happens on the boundaries of the grid cell along the y -axis, the x -axis, and the x - and y -axes at the same time, respectively. Based on Eqs. (3), (4), and (6), and adding an extra $\int_0^{\pi/2} d\psi$ to each term of Eqs.(48)-(50), we have

$$S_{\text{coll}}^{3\text{D}}(x) = b \int_0^{\frac{\pi}{2}} d\psi \int_0^{\pi} d\phi \int_0^{a-\sigma} \Theta(|l \sin \psi \cos \phi| - x) dx + \sigma b \frac{\pi^2}{2}. \quad (133)$$

$$S_{\text{coll}}^{3\text{D}}(y) = a \int_0^{\frac{\pi}{2}} d\psi \int_0^{\pi} d\phi \int_0^{b-\sigma} \Theta(l \sin \psi \sin \phi - y) dy + \sigma a \frac{\pi^2}{2}, \quad (134)$$

$$\begin{aligned} S_{\text{coll}}^{3\text{D}}(x, y) &= \int_0^{\frac{\pi}{2}} d\psi \int_0^{\pi} d\phi \int_0^{a-\sigma} \Theta(|l \sin \psi \cos \phi| - x) dx \int_0^{b-\sigma} \Theta(l \sin \psi \sin \phi - y) dy \\ &\quad + \sigma \int_0^{\frac{\pi}{2}} d\psi \int_0^{\pi} d\phi \int_0^{a-\sigma} \Theta(|l \sin \psi \cos \phi| - x) dx + \sigma \int_0^{\frac{\pi}{2}} d\psi \int_0^{\pi} d\phi \int_0^{b-\sigma} \Theta(l \sin \psi \sin \phi - y) dy \\ &\quad + \sigma^2 \frac{\pi^2}{2}. \end{aligned} \quad (135)$$

With the definitions in Eqs.(81)-(83), we have

$$S_{\text{coll}}^{3\text{D}}(x) = bA^{3\text{D}}(l, a - \sigma) + \sigma b \frac{\pi^2}{2}, \quad (136)$$

$$S_{\text{coll}}^{3\text{D}}(y) = aB^{3\text{D}}(l, b - \sigma) + \sigma a \frac{\pi^2}{2}, \quad (137)$$

$$S_{\text{coll}}^{3\text{D}}(x, y) = AB^{3\text{D}}(l, a - \sigma, b - \sigma) + \sigma A^{3\text{D}}(l, a - \sigma) + \sigma B^{3\text{D}}(l, b - \sigma) + \sigma^2 \frac{\pi^2}{2}. \quad (138)$$

Equivalently, we have

$$S_{\text{coll}}^{3\text{D}} = (b - \sigma)A^{3\text{D}}(l, a - \sigma) + (a - \sigma)B^{3\text{D}}(l, b - \sigma) - AB^{3\text{D}}(l, a - \sigma, b - \sigma) + (\sigma a + \sigma b - \sigma^2) \frac{\pi^2}{2}. \quad (139)$$

With the results of $A^{3\text{D}}(l, a)$, $B^{3\text{D}}(l, b)$ and $AB^{3\text{D}}(l, a, b)$ in Sec.V, we can easily lay down those of Eq.(139). Before that, as Eqs.(86), (92), and (112) defined for the BLNP with 3D needles, we define their respective version for the BLNP with 3D spherocylinders as

$$\hat{\psi}_x^* = \arcsin \frac{a - \sigma}{l}, \quad (140)$$

$$\hat{\psi}_y^* = \arcsin \frac{b - \sigma}{l}, \quad (141)$$

$$\hat{\psi}_{xy}^* = \arcsin \frac{\hat{L}}{l}. \quad (142)$$

When $l \leq b - \sigma$, with Eq. (139) we have

$$\begin{aligned} S_{\text{coll}}^{3\text{D}} &= (b - \sigma)A^{3\text{D}}(l, a - \sigma | l \leq a - \sigma) + (a - \sigma)B^{3\text{D}}(l, b - \sigma | l \leq b - \sigma) \\ &\quad - AB^{3\text{D}}(l, a - \sigma, b - \sigma | l \leq b - \sigma) + (\sigma a + \sigma b - \sigma^2) \frac{\pi^2}{2} \\ &= 2l(b - \sigma) + 2l(a - \sigma) - \frac{\pi}{4}l^2 + (\sigma a + \sigma b - \sigma^2) \frac{\pi^2}{2}. \end{aligned} \quad (143)$$

Then,

$$P^{3\text{D}}(l, \sigma, a, b) = \frac{4}{\pi^2} \frac{b - \sigma}{b} \frac{l}{a} + \frac{4}{\pi^2} \frac{a - \sigma}{a} \frac{l}{b} - \frac{1}{2\pi} \frac{l^2}{ab} + \left(\frac{\sigma}{a} + \frac{\sigma}{b} - \frac{\sigma^2}{ab} \right). \quad (144)$$

When $b - \sigma < l \leq a - \sigma$, we have

$$\begin{aligned} S_{\text{coll}}^{3\text{D}} &= (b - \sigma)A^{3\text{D}}(l, a - \sigma | l \leq a - \sigma) + (a - \sigma)B^{3\text{D}}(l, b - \sigma | b - \sigma < l) \\ &\quad - AB^{3\text{D}}(l, a - \sigma, b - \sigma | b - \sigma < l \leq a - \sigma) + (\sigma a + \sigma b - \sigma^2) \frac{\pi^2}{2} \\ &= 2l(b - \sigma) + \left[2l(a - \sigma) - 2l(a - \sigma)F\left(\hat{\psi}_y^*, \frac{\pi}{2}, \frac{b - \sigma}{l}\right) + 2(a - \sigma)(b - \sigma)G\left(\hat{\psi}_y^*, \frac{\pi}{2}, \frac{b - \sigma}{l}\right) \right] \\ &\quad - \left[\frac{l^2}{2} \hat{\psi}_y^* + \frac{3}{2}l(b - \sigma) \cos \hat{\psi}_y^* - (b - \sigma)^2 \left(\frac{\pi}{2} - \hat{\psi}_y^* \right) \right] + (\sigma a + \sigma b - \sigma^2) \frac{\pi^2}{2} \\ &= 2l(b - \sigma) + \left[2l(a - \sigma) - 2l(a - \sigma)F\left(\arcsin \frac{b - \sigma}{l}, \frac{\pi}{2}, \frac{b - \sigma}{l}\right) + 2(a - \sigma)(b - \sigma)G\left(\arcsin \frac{b - \sigma}{l}, \frac{\pi}{2}, \frac{b - \sigma}{l}\right) \right] \\ &\quad - \left[\frac{l^2}{2} \arcsin \frac{b - \sigma}{l} + \frac{3}{2}l(b - \sigma) \sqrt{1 - \frac{(b - \sigma)^2}{l^2}} - (b - \sigma)^2 \left(\frac{\pi}{2} - \arcsin \frac{b - \sigma}{l} \right) \right] + (\sigma a + \sigma b - \sigma^2) \frac{\pi^2}{2}. \end{aligned} \quad (145)$$

Then,

$$\begin{aligned} P^{3\text{D}}(l, \sigma, a, b) &= \frac{4}{\pi^2} \frac{b - \sigma}{b} \frac{l}{a} + \left[\frac{4}{\pi^2} \frac{a - \sigma}{a} \frac{l}{b} - \frac{4}{\pi^2} \frac{a - \sigma}{a} \frac{l}{b} F\left(\arcsin \frac{b - \sigma}{l}, \frac{\pi}{2}, \frac{b - \sigma}{l}\right) + \frac{4}{\pi^2} \frac{a - \sigma}{a} \frac{b - \sigma}{b} G\left(\arcsin \frac{b - \sigma}{l}, \frac{\pi}{2}, \frac{b - \sigma}{l}\right) \right] \\ &\quad - \left[\frac{1}{\pi^2} \frac{l^2}{ab} \arcsin \frac{b - \sigma}{l} + \frac{3}{\pi^2} \frac{b - \sigma}{b} \frac{l}{a} \sqrt{1 - \frac{(b - \sigma)^2}{l^2}} - \frac{2}{\pi^2} \frac{(b - \sigma)^2}{ab} \left(\frac{\pi}{2} - \arcsin \frac{b - \sigma}{l} \right) \right] + \left(\frac{\sigma}{a} + \frac{\sigma}{b} - \frac{\sigma^2}{ab} \right). \end{aligned} \quad (146)$$

When $a - \sigma < l \leq \hat{L}$, we have

$$\begin{aligned}
S_{\text{coll}}^{3\text{D}} &= (b - \sigma)A^{3\text{D}}(l, a - \sigma | a - \sigma < l) + (a - \sigma)B^{3\text{D}}(l, b - \sigma | b - \sigma < l) \\
&\quad - AB^{3\text{D}}(l, a - \sigma, b - \sigma | a - \sigma < l \leq \hat{L}) + (\sigma a + \sigma b - \sigma^2) \frac{\pi^2}{2} \\
&= \left[2l(b - \sigma) - 2l(b - \sigma)F\left(\hat{\psi}_x^*, \frac{\pi}{2}, \frac{a - \sigma}{l}\right) + 2(a - \sigma)(b - \sigma)G\left(\hat{\psi}_x^*, \frac{\pi}{2}, \frac{a - \sigma}{l}\right) \right] \\
&\quad + \left[2l(a - \sigma) - 2l(a - \sigma)F\left(\hat{\psi}_y^*, \frac{\pi}{2}, \frac{b - \sigma}{l}\right) + 2(a - \sigma)(b - \sigma)G\left(\hat{\psi}_y^*, \frac{\pi}{2}, \frac{b - \sigma}{l}\right) \right] \\
&\quad - \left[\frac{l^2}{2}\hat{\psi}_x^* + \frac{3}{2}l(a - \sigma)\cos\hat{\psi}_x^* - (a - \sigma)^2\left(\frac{\pi}{2} - \hat{\psi}_x^*\right) \right] \\
&\quad - \left[\frac{l^2}{2}\hat{\psi}_y^* + \frac{3}{2}l(b - \sigma)\cos\hat{\psi}_y^* - (b - \sigma)^2\left(\frac{\pi}{2} - \hat{\psi}_y^*\right) \right] \\
&\quad + \frac{\pi}{4}l^2 + (\sigma a + \sigma b - \sigma^2) \frac{\pi^2}{2} \\
&= \left[2l(b - \sigma) - 2l(b - \sigma)F\left(\arcsin\frac{a - \sigma}{l}, \frac{\pi}{2}, \frac{a - \sigma}{l}\right) + 2(a - \sigma)(b - \sigma)G\left(\arcsin\frac{a - \sigma}{l}, \frac{\pi}{2}, \frac{a - \sigma}{l}\right) \right] \\
&\quad + \left[2l(a - \sigma) - 2l(a - \sigma)F\left(\arcsin\frac{b - \sigma}{l}, \frac{\pi}{2}, \frac{b - \sigma}{l}\right) + 2(a - \sigma)(b - \sigma)G\left(\arcsin\frac{b - \sigma}{l}, \frac{\pi}{2}, \frac{b - \sigma}{l}\right) \right] \\
&\quad - \left[\frac{l^2}{2}\arcsin\frac{a - \sigma}{l} + \frac{3}{2}l(a - \sigma)\sqrt{1 - \frac{(a - \sigma)^2}{l^2}} - (a - \sigma)^2\left(\frac{\pi}{2} - \arcsin\frac{a - \sigma}{l}\right) \right] \\
&\quad - \left[\frac{l^2}{2}\arcsin\frac{b - \sigma}{l} + \frac{3}{2}l(b - \sigma)\sqrt{1 - \frac{(b - \sigma)^2}{l^2}} - (b - \sigma)^2\left(\frac{\pi}{2} - \arcsin\frac{b - \sigma}{l}\right) \right] \\
&\quad + \frac{\pi}{4}l^2 + (\sigma a + \sigma b - \sigma^2) \frac{\pi^2}{2}. \tag{147}
\end{aligned}$$

Then,

$$\begin{aligned}
P^{3\text{D}}(l, \sigma, a, b) &= \left[\frac{4}{\pi^2} \frac{b - \sigma}{b} \frac{l}{a} - \frac{4}{\pi^2} \frac{b - \sigma}{b} \frac{l}{a} F\left(\arcsin\frac{a - \sigma}{l}, \frac{\pi}{2}, \frac{a - \sigma}{l}\right) + \frac{4}{\pi^2} \frac{a - \sigma}{a} \frac{b - \sigma}{b} G\left(\arcsin\frac{a - \sigma}{l}, \frac{\pi}{2}, \frac{a - \sigma}{l}\right) \right] \\
&\quad + \left[\frac{4}{\pi^2} \frac{a - \sigma}{a} \frac{l}{b} - \frac{4}{\pi^2} \frac{a - \sigma}{a} \frac{l}{b} F\left(\arcsin\frac{b - \sigma}{l}, \frac{\pi}{2}, \frac{b - \sigma}{l}\right) + \frac{4}{\pi^2} \frac{a - \sigma}{a} \frac{b - \sigma}{b} G\left(\arcsin\frac{b - \sigma}{l}, \frac{\pi}{2}, \frac{b - \sigma}{l}\right) \right] \\
&\quad - \left[\frac{1}{\pi^2} \frac{l^2}{ab} \arcsin\frac{a - \sigma}{l} + \frac{3}{\pi^2} \frac{a - \sigma}{a} \frac{l}{b} \sqrt{1 - \frac{(a - \sigma)^2}{l^2}} - \frac{2}{\pi^2} \frac{(a - \sigma)^2}{ab} \left(\frac{\pi}{2} - \arcsin\frac{a - \sigma}{l}\right) \right] \\
&\quad - \left[\frac{1}{\pi^2} \frac{l^2}{ab} \arcsin\frac{b - \sigma}{l} + \frac{3}{\pi^2} \frac{b - \sigma}{b} \frac{l}{a} \sqrt{1 - \frac{(b - \sigma)^2}{l^2}} - \frac{2}{\pi^2} \frac{(b - \sigma)^2}{ab} \left(\frac{\pi}{2} - \arcsin\frac{b - \sigma}{l}\right) \right] \\
&\quad + \frac{1}{2\pi} \frac{l^2}{ab} + \left(\frac{\sigma}{a} + \frac{\sigma}{b} - \frac{\sigma^2}{ab}\right). \tag{148}
\end{aligned}$$

When $\hat{L} < l$, we have

$$\begin{aligned}
S_{\text{coll}}^{3\text{D}} &= (b - \sigma)A^{3\text{D}}(l, a - \sigma | a - \sigma < l) + (a - \sigma)B^{3\text{D}}(l, b - \sigma | b - \sigma < l) \\
&\quad - AB^{3\text{D}}(l, a - \sigma, b - \sigma | \hat{L} < l) + (\sigma a + \sigma b - \sigma^2) \frac{\pi^2}{2} \\
&= \left[2l(b - \sigma) - 2l(b - \sigma)F\left(\hat{\psi}_x^*, \hat{\psi}_{xy}^*, \frac{a - \sigma}{l}\right) + 2(a - \sigma)(b - \sigma)G\left(\hat{\psi}_x^*, \hat{\psi}_{xy}^*, \frac{a - \sigma}{l}\right) \right] \\
&\quad + \left[2l(a - \sigma) - 2l(a - \sigma)F\left(\hat{\psi}_y^*, \hat{\psi}_{xy}^*, \frac{b - \sigma}{l}\right) + 2(a - \sigma)(b - \sigma)G\left(\hat{\psi}_y^*, \hat{\psi}_{xy}^*, \frac{b - \sigma}{l}\right) \right] \\
&\quad - \left[\frac{l^2}{2}\hat{\psi}_x^* + \frac{3}{2}l(a - \sigma)\cos\hat{\psi}_x^* - (a - \sigma)^2\left(\frac{\pi}{2} - \hat{\psi}_x^*\right) \right]
\end{aligned}$$

$$\begin{aligned}
& - \left[\frac{l^2}{2} \hat{\psi}_y^* + \frac{3}{2} l(b-\sigma) \cos \hat{\psi}_y^* - (b-\sigma)^2 \left(\frac{\pi}{2} - \hat{\psi}_y^* \right) \right] \\
& + \left[\frac{l^2}{2} \hat{\psi}_{xy}^* - \frac{l\hat{L}}{2} \cos \hat{\psi}_{xy}^* - \hat{L}^2 \left(\frac{\pi}{2} - \hat{\psi}_{xy}^* \right) \right] \\
& + (a-\sigma)(b-\sigma)\pi \left(\frac{\pi}{2} - \hat{\psi}_{xy}^* \right) + (\sigma a + \sigma b - \sigma^2) \frac{\pi^2}{2} \\
& = \left[2l(b-\sigma) - 2l(b-\sigma)F \left(\arcsin \frac{a-\sigma}{l}, \arcsin \frac{\hat{L}}{l}, \frac{a-\sigma}{l} \right) + 2(a-\sigma)(b-\sigma)G \left(\arcsin \frac{a-\sigma}{l}, \arcsin \frac{\hat{L}}{l}, \frac{a-\sigma}{l} \right) \right] \\
& + \left[2l(a-\sigma) - 2l(a-\sigma)F \left(\arcsin \frac{b-\sigma}{l}, \arcsin \frac{\hat{L}}{l}, \frac{b-\sigma}{l} \right) + 2(a-\sigma)(b-\sigma)G \left(\arcsin \frac{b-\sigma}{l}, \arcsin \frac{\hat{L}}{l}, \frac{b-\sigma}{l} \right) \right] \\
& - \left[\frac{l^2}{2} \arcsin \frac{a-\sigma}{l} + \frac{3}{2} l(a-\sigma) \sqrt{1 - \frac{(a-\sigma)^2}{l^2}} - (a-\sigma)^2 \left(\frac{\pi}{2} - \arcsin \frac{a-\sigma}{l} \right) \right] \\
& - \left[\frac{l^2}{2} \arcsin \frac{b-\sigma}{l} + \frac{3}{2} l(b-\sigma) \sqrt{1 - \frac{(b-\sigma)^2}{l^2}} - (b-\sigma)^2 \left(\frac{\pi}{2} - \arcsin \frac{b-\sigma}{l} \right) \right] \\
& + \left[\frac{l^2}{2} \arcsin \frac{\hat{L}}{l} - \frac{l\hat{L}}{2} \sqrt{1 - \frac{\hat{L}^2}{l^2}} - \hat{L}^2 \left(\frac{\pi}{2} - \arcsin \frac{\hat{L}}{l} \right) \right] \\
& + (a-\sigma)(b-\sigma)\pi \left(\frac{\pi}{2} - \arcsin \frac{\hat{L}}{l} \right) + (\sigma a + \sigma b - \sigma^2) \frac{\pi^2}{2}. \tag{149}
\end{aligned}$$

Then,

$$\begin{aligned}
& P^{3D}(l, \sigma, a, b) \\
& = \left[\frac{4}{\pi^2} \frac{b-\sigma}{b} \frac{l}{a} - \frac{4}{\pi^2} \frac{b-\sigma}{b} \frac{l}{a} F \left(\arcsin \frac{a-\sigma}{l}, \arcsin \frac{\hat{L}}{l}, \frac{a-\sigma}{l} \right) + \frac{4}{\pi^2} \frac{a-\sigma}{a} \frac{b-\sigma}{b} G \left(\arcsin \frac{a-\sigma}{l}, \arcsin \frac{\hat{L}}{l}, \frac{a-\sigma}{l} \right) \right] \\
& + \left[\frac{4}{\pi^2} \frac{a-\sigma}{a} \frac{l}{b} - \frac{4}{\pi^2} \frac{a-\sigma}{a} \frac{l}{b} F \left(\arcsin \frac{b-\sigma}{l}, \arcsin \frac{\hat{L}}{l}, \frac{b-\sigma}{l} \right) + \frac{4}{\pi^2} \frac{a-\sigma}{a} \frac{b-\sigma}{b} G \left(\arcsin \frac{b-\sigma}{l}, \arcsin \frac{\hat{L}}{l}, \frac{b-\sigma}{l} \right) \right] \\
& - \left[\frac{1}{\pi^2} \frac{l^2}{ab} \arcsin \frac{a-\sigma}{l} + \frac{3}{\pi^2} \frac{a-\sigma}{a} \frac{l}{b} \sqrt{1 - \frac{(a-\sigma)^2}{l^2}} - \frac{2}{\pi^2} \frac{(a-\sigma)^2}{ab} \left(\frac{\pi}{2} - \arcsin \frac{a-\sigma}{l} \right) \right] \\
& - \left[\frac{1}{\pi^2} \frac{l^2}{ab} \arcsin \frac{b-\sigma}{l} + \frac{3}{\pi^2} \frac{b-\sigma}{b} \frac{l}{a} \sqrt{1 - \frac{(b-\sigma)^2}{l^2}} - \frac{2}{\pi^2} \frac{(b-\sigma)^2}{ab} \left(\frac{\pi}{2} - \arcsin \frac{b-\sigma}{l} \right) \right] \\
& + \left[\frac{1}{\pi^2} \frac{l^2}{ab} \arcsin \frac{\hat{L}}{l} - \frac{1}{\pi^2} \frac{l\hat{L}}{ab} \sqrt{1 - \frac{\hat{L}^2}{l^2}} - \frac{2}{\pi^2} \frac{\hat{L}^2}{ab} \left(\frac{\pi}{2} - \arcsin \frac{\hat{L}}{l} \right) \right] \\
& + \frac{2}{\pi} \frac{a-\sigma}{a} \frac{b-\sigma}{b} \left(\frac{\pi}{2} - \arcsin \frac{\hat{L}}{l} \right) + \left(\frac{\sigma}{a} + \frac{\sigma}{b} - \frac{\sigma^2}{ab} \right). \tag{150}
\end{aligned}$$

Summing up the results in Eqs.(144), (146), (148), and (150), we have

$$P^{3D}(l, \sigma, a, b) =$$

$$\left\{ \begin{array}{l}
\frac{4}{\pi^2} \frac{b-\sigma}{b} \frac{l}{a} + \frac{4}{\pi^2} \frac{a-\sigma}{a} \frac{l}{b} - \frac{1}{2\pi} \frac{l^2}{ab} + \left(\frac{\sigma}{a} + \frac{\sigma}{b} - \frac{\sigma^2}{ab} \right), \quad \text{if } l \leq b - \sigma; \\
\frac{4}{\pi^2} \frac{b-\sigma}{b} \frac{l}{a} + \left[\frac{4}{\pi^2} \frac{a-\sigma}{a} \frac{l}{b} - \frac{4}{\pi^2} \frac{a-\sigma}{a} \frac{l}{b} F \left(\arcsin \frac{b-\sigma}{l}, \frac{\pi}{2}, \frac{b-\sigma}{l} \right) + \frac{4}{\pi^2} \frac{a-\sigma}{a} \frac{b-\sigma}{b} G \left(\arcsin \frac{b-\sigma}{l}, \frac{\pi}{2}, \frac{b-\sigma}{l} \right) \right] \\
- \left[\frac{1}{\pi^2} \frac{l^2}{ab} \arcsin \frac{b-\sigma}{l} + \frac{3}{\pi^2} \frac{b-\sigma}{b} \frac{l}{a} \sqrt{1 - \frac{(b-\sigma)^2}{l^2}} - \frac{2}{\pi^2} \frac{(b-\sigma)^2}{ab} \left(\frac{\pi}{2} - \arcsin \frac{b-\sigma}{l} \right) \right] + \left(\frac{\sigma}{a} + \frac{\sigma}{b} - \frac{\sigma^2}{ab} \right), \quad \text{if } b - \sigma < l \leq a - \sigma; \\
\left[\frac{4}{\pi^2} \frac{b-\sigma}{b} \frac{l}{a} - \frac{4}{\pi^2} \frac{b-\sigma}{b} \frac{l}{a} F \left(\arcsin \frac{a-\sigma}{l}, \frac{\pi}{2}, \frac{a-\sigma}{l} \right) + \frac{4}{\pi^2} \frac{a-\sigma}{a} \frac{b-\sigma}{b} G \left(\arcsin \frac{a-\sigma}{l}, \frac{\pi}{2}, \frac{a-\sigma}{l} \right) \right] \\
+ \left[\frac{4}{\pi^2} \frac{a-\sigma}{a} \frac{l}{b} - \frac{4}{\pi^2} \frac{a-\sigma}{a} \frac{l}{b} F \left(\arcsin \frac{b-\sigma}{l}, \frac{\pi}{2}, \frac{b-\sigma}{l} \right) + \frac{4}{\pi^2} \frac{a-\sigma}{a} \frac{b-\sigma}{b} G \left(\arcsin \frac{b-\sigma}{l}, \frac{\pi}{2}, \frac{b-\sigma}{l} \right) \right] \\
- \left[\frac{1}{\pi^2} \frac{l^2}{ab} \arcsin \frac{a-\sigma}{l} + \frac{3}{\pi^2} \frac{a-\sigma}{a} \frac{l}{b} \sqrt{1 - \frac{(a-\sigma)^2}{l^2}} - \frac{2}{\pi^2} \frac{(a-\sigma)^2}{ab} \left(\frac{\pi}{2} - \arcsin \frac{a-\sigma}{l} \right) \right] \\
- \left[\frac{1}{\pi^2} \frac{l^2}{ab} \arcsin \frac{b-\sigma}{l} + \frac{3}{\pi^2} \frac{b-\sigma}{b} \frac{l}{a} \sqrt{1 - \frac{(b-\sigma)^2}{l^2}} - \frac{2}{\pi^2} \frac{(b-\sigma)^2}{ab} \left(\frac{\pi}{2} - \arcsin \frac{b-\sigma}{l} \right) \right] \\
+ \frac{1}{2\pi} \frac{l^2}{ab} + \left(\frac{\sigma}{a} + \frac{\sigma}{b} - \frac{\sigma^2}{ab} \right), \quad \text{if } a - \sigma < l \leq \hat{L} \quad (151) \\
\left[\frac{4}{\pi^2} \frac{b-\sigma}{b} \frac{l}{a} - \frac{4}{\pi^2} \frac{b-\sigma}{b} \frac{l}{a} F \left(\arcsin \frac{a-\sigma}{l}, \arcsin \frac{\hat{L}}{l}, \frac{a-\sigma}{l} \right) + \frac{4}{\pi^2} \frac{a-\sigma}{a} \frac{b-\sigma}{b} G \left(\arcsin \frac{a-\sigma}{l}, \arcsin \frac{\hat{L}}{l}, \frac{a-\sigma}{l} \right) \right] \\
+ \left[\frac{4}{\pi^2} \frac{a-\sigma}{a} \frac{l}{b} - \frac{4}{\pi^2} \frac{a-\sigma}{a} \frac{l}{b} F \left(\arcsin \frac{b-\sigma}{l}, \arcsin \frac{\hat{L}}{l}, \frac{b-\sigma}{l} \right) + \frac{4}{\pi^2} \frac{a-\sigma}{a} \frac{b-\sigma}{b} G \left(\arcsin \frac{b-\sigma}{l}, \arcsin \frac{\hat{L}}{l}, \frac{b-\sigma}{l} \right) \right] \\
- \left[\frac{1}{\pi^2} \frac{l^2}{ab} \arcsin \frac{a-\sigma}{l} + \frac{3}{\pi^2} \frac{a-\sigma}{a} \frac{l}{b} \sqrt{1 - \frac{(a-\sigma)^2}{l^2}} - \frac{2}{\pi^2} \frac{(a-\sigma)^2}{ab} \left(\frac{\pi}{2} - \arcsin \frac{a-\sigma}{l} \right) \right] \\
- \left[\frac{1}{\pi^2} \frac{l^2}{ab} \arcsin \frac{b-\sigma}{l} + \frac{3}{\pi^2} \frac{b-\sigma}{b} \frac{l}{a} \sqrt{1 - \frac{(b-\sigma)^2}{l^2}} - \frac{2}{\pi^2} \frac{(b-\sigma)^2}{ab} \left(\frac{\pi}{2} - \arcsin \frac{b-\sigma}{l} \right) \right] \\
+ \left[\frac{1}{\pi^2} \frac{l^2}{ab} \arcsin \frac{\hat{L}}{l} - \frac{1}{\pi^2} \frac{l\hat{L}}{ab} \sqrt{1 - \frac{\hat{L}^2}{l^2}} - \frac{2}{\pi^2} \frac{\hat{L}^2}{ab} \left(\frac{\pi}{2} - \arcsin \frac{\hat{L}}{l} \right) \right] \\
+ \frac{2}{\pi} \frac{a-\sigma}{a} \frac{b-\sigma}{b} \left(\frac{\pi}{2} - \arcsin \frac{\hat{L}}{l} \right) + \left(\frac{\sigma}{a} + \frac{\sigma}{b} - \frac{\sigma^2}{ab} \right), \quad \text{if } \hat{L} < l.
\end{array} \right.$$

When $l/a \rightarrow 0$, Eqs. (144) and (146) simplify to the result for the BNP of 3D spherocylinders as

$$P^{3D}(l, \sigma, \infty, b) = \begin{cases} \frac{4}{\pi^2} \frac{l}{b} + \frac{\sigma}{b}, & \text{if } l \leq b - \sigma; \\ \frac{4}{\pi^2} \frac{l}{b} - \frac{4}{\pi^2} \frac{l}{b} F \left(\arcsin \frac{b-\sigma}{l}, \frac{\pi}{2}, \frac{b-\sigma}{l} \right) + \frac{4}{\pi^2} \frac{b-\sigma}{b} G \left(\arcsin \frac{b-\sigma}{l}, \frac{\pi}{2}, \frac{b-\sigma}{l} \right) + \frac{\sigma}{b}, & \text{if } b - \sigma < l. \end{cases} \quad (152)$$

We further check the consistency of Eq.(151) on its boundaries of four cases of $P^{3D}(l, \sigma, a, b)$, equivalently S_{coll}^{3D} . When $l = 0$, based on the case of $l \leq b$, we have

$$S_{\text{coll}}^{3D} = (\sigma a + \sigma b - \sigma^2) \frac{\pi^2}{2}, \quad (153)$$

which is simply S_{coll} in Eq. (70) for the problem of 2D spherocylinders with $l = 0$, multiplying by the range of the new degree of freedom ψ , or $\pi/2$.

When $l = b - \sigma$, both the cases of $l \leq b - \sigma$ and $b - \sigma < l \leq a - \sigma$ reduce to

$$S_{\text{coll}}^{3D} = \left(2 - \frac{\pi}{4} \right) (b - \sigma)^2 + 2(a - \sigma)(b - \sigma) + (\sigma a + \sigma b - \sigma^2) \frac{\pi^2}{2}. \quad (154)$$

When $l = a - \sigma$, both the cases of $b - \sigma < l \leq a - \sigma$ and $a - \sigma < l \leq \hat{L}$ correspond to

$$\begin{aligned}
S_{\text{coll}}^{3D} &= 2(a - \sigma)(b - \sigma) \\
&+ \left[2(a - \sigma)^2 - 2(a - \sigma)^2 F \left(\arcsin \frac{b - \sigma}{a - \sigma}, \frac{\pi}{2}, \frac{b - \sigma}{a - \sigma} \right) + 2(a - \sigma)(b - \sigma) G \left(\arcsin \frac{b - \sigma}{a - \sigma}, \frac{\pi}{2}, \frac{b - \sigma}{a - \sigma} \right) \right] \\
&- \left[\frac{(a - \sigma)^2}{2} \arcsin \frac{b - \sigma}{a - \sigma} + \frac{3}{2} (a - \sigma)(b - \sigma) \sqrt{1 - \frac{(b - \sigma)^2}{(a - \sigma)^2}} - (b - \sigma)^2 \left(\frac{\pi}{2} - \arcsin \frac{b - \sigma}{a - \sigma} \right) \right] \\
&+ (\sigma a + \sigma b - \sigma^2) \frac{\pi^2}{2}. \quad (155)
\end{aligned}$$

When $l = \hat{L}$, both the cases of $a - \sigma < l \leq \hat{L}$ and $\hat{L} < l$ result in

$$\begin{aligned}
S_{\text{coll}}^{3\text{D}} &= \left[2\hat{L}(b - \sigma) - 2\hat{L}(b - \sigma)F\left(\arcsin \frac{a - \sigma}{\hat{L}}, \frac{\pi}{2}, \frac{a - \sigma}{\hat{L}}\right) + 2(a - \sigma)(b - \sigma)G\left(\arcsin \frac{a - \sigma}{\hat{L}}, \frac{\pi}{2}, \frac{a - \sigma}{\hat{L}}\right) \right] \\
&+ \left[2\hat{L}(a - \sigma) - 2\hat{L}(a - \sigma)F\left(\arcsin \frac{b - \sigma}{\hat{L}}, \frac{\pi}{2}, \frac{b - \sigma}{\hat{L}}\right) + 2(a - \sigma)(b - \sigma)G\left(\arcsin \frac{b - \sigma}{\hat{L}}, \frac{\pi}{2}, \frac{b - \sigma}{\hat{L}}\right) \right] \\
&- \left[3(a - \sigma)(b - \sigma) - (a - \sigma)^2 \left(\frac{\pi}{2} - \arcsin \frac{a - \sigma}{\hat{L}}\right) - (b - \sigma)^2 \left(\frac{\pi}{2} - \arcsin \frac{b - \sigma}{\hat{L}}\right) \right] \\
&+ (\sigma a + \sigma b - \sigma^2) \frac{\pi^2}{2}.
\end{aligned} \tag{156}$$

Finally, we consider the limit case of $l \rightarrow \infty$. With Eqs.(127)-(130) and substituting (a, b) with $(a - \sigma, b - \sigma)$ respectively, we have

$$l(b - \sigma)F\left(\arcsin \frac{a - \sigma}{l}, \arcsin \frac{\hat{L}}{l}, \frac{a - \sigma}{l}\right) \sim \frac{1}{2}(b - \sigma)^2 \left(\arcsin \frac{\hat{L}}{l} - \arcsin \frac{a - \sigma}{l}\right) \rightarrow 0, \tag{157}$$

$$l(a - \sigma)F\left(\arcsin \frac{b - \sigma}{l}, \arcsin \frac{\hat{L}}{l}, \frac{b - \sigma}{l}\right) \sim \frac{1}{2}(a - \sigma)^2 \left(\arcsin \frac{\hat{L}}{l} - \arcsin \frac{b - \sigma}{l}\right) \rightarrow 0, \tag{158}$$

$$G\left(\arcsin \frac{a - \sigma}{l}, \arcsin \frac{\hat{L}}{l}, \frac{a - \sigma}{l}\right) \sim \frac{1}{2} \left(\arcsin \frac{\hat{L}}{l} - \arcsin \frac{a - \sigma}{l}\right) \left(\frac{\pi}{2} - \arcsin \frac{a - \sigma}{\hat{L}}\right) \rightarrow 0, \tag{159}$$

$$G\left(\arcsin \frac{b - \sigma}{l}, \arcsin \frac{\hat{L}}{l}, \frac{b - \sigma}{l}\right) \sim \frac{1}{2} \left(\arcsin \frac{\hat{L}}{l} - \arcsin \frac{b - \sigma}{l}\right) \left(\frac{\pi}{2} - \arcsin \frac{b - \sigma}{\hat{L}}\right) \rightarrow 0. \tag{160}$$

Thus Eq.(149) reduces to

$$\begin{aligned}
S_{\text{coll}}^{3\text{D}} &= [2l(b - \sigma) - 2 \cdot 0 + 2(a - \sigma)(b - \sigma) \cdot 0] \\
&+ [2l(a - \sigma) - 2 \cdot 0 + 2(a - \sigma)(b - \sigma) \cdot 0] \\
&- \left[\frac{l^2}{2} \cdot \frac{a - \sigma}{l} + \frac{3}{2}l(a - \sigma) \cdot \sqrt{1 - 0} - (a - \sigma)^2 \cdot \left(\frac{\pi}{2} - 0\right) \right] \\
&- \left[\frac{l^2}{2} \cdot \frac{b - \sigma}{l} + \frac{3}{2}l(b - \sigma) \cdot \sqrt{1 - 0} - (b - \sigma)^2 \cdot \left(\frac{\pi}{2} - 0\right) \right] \\
&+ \left[\frac{l^2}{2} \cdot \frac{\hat{L}}{l} - \frac{l\hat{L}}{2} \cdot \sqrt{1 - 0} - \hat{L}^2 \cdot \left(\frac{\pi}{2} - 0\right) \right] \\
&+ (a - \sigma)(b - \sigma)\pi \cdot \left(\frac{\pi}{2} - 0\right) + (\sigma a + \sigma b - \sigma^2) \frac{\pi^2}{2} \\
&= ab \frac{\pi^2}{2}.
\end{aligned} \tag{161}$$

Equivalently, $P^{3\text{D}}(\infty, \sigma, a, b) = 1$. This is just like the case of infinitely long 3D needles: only a 3D spherocylinder with an infinitely large length intersect with a grid with a probability of 1.

VII. RESULT

Our analytical result summed in Eqs.(40), (41), (68), (69), (121), (122), (151), and (152) only depend on the relative sizes of objects, say l , σ , a , and b . To verify their correctness, we perform Monte Carlo simulation of dropping objects for given finite l , σ , a , and b explained in Sec.II, and compare these empirical intersection probability with theoretical predictions from our analytical

framework.

To numerically calculate integrals, there is a large toolbox in existing literature we can refer to. Here for simplicity we adopt the classical Simpson's rule [17] for Eqs. (89) and (90). We can see that the integrands in both integrals have a closed form. We divide the range $[a, b]$ into equally spaced intervals with a size $[(b - a) \times N_{\text{unit}} \times 2i]$ with $i = 1, 2, \dots$, and calculate a sequence of numerical summations $F(i)$ based on Simpson's rule. When $|F(i + 1) - F(i)| < \varepsilon$, we consider $F(i + 1)$ as our numer-

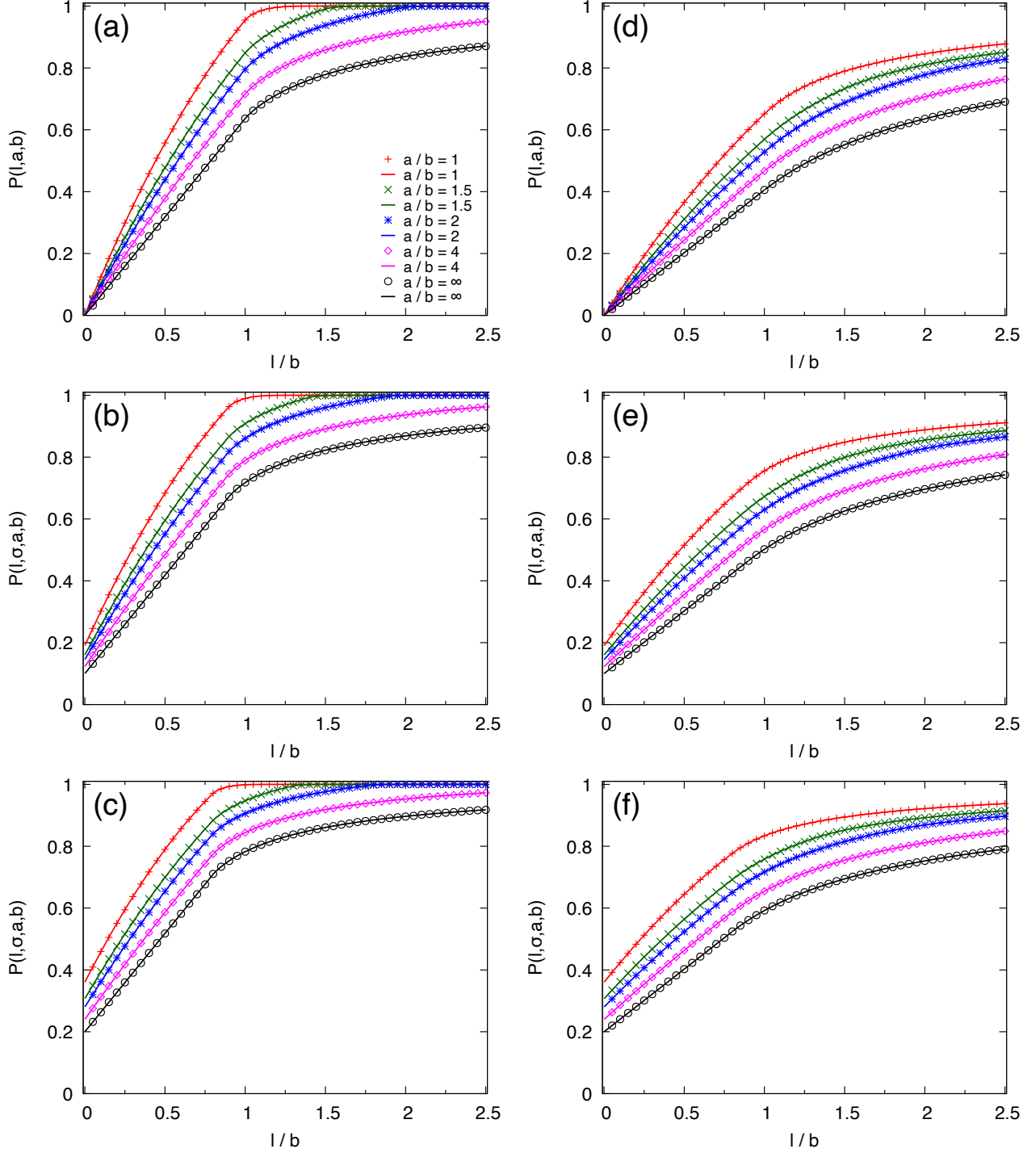


FIG. 4. Result of BLNP with needles and spherocylinders with fixed height b of a grid cell. (a) The intersection probability $P(l, a, b)$ versus the ratio l/b is shown in the case of 2D needles. (b)-(c) The intersection probability $P(l, \sigma, a, b)$ versus l/b is shown in the case of 2D spherocylinders with $\sigma/b = 0.1$ and 0.2 , respectively. (d)-(f) Results are shown in the same format as (a)-(c), yet for the case of 3D needles and spherocylinders. In each subfigure, we show results when $a/b = 1, 1.5, 2, 4, \infty$, the last of which simply corresponds to the BNP version. Each sign is from result of a single Monte Carlo simulation with $b = 3$ and a configuration size $N_{\text{all}} = 10^6$ for the 2D case and $N_{\text{all}} = 10^7$ for the 3D case. Lines are from analytical results.

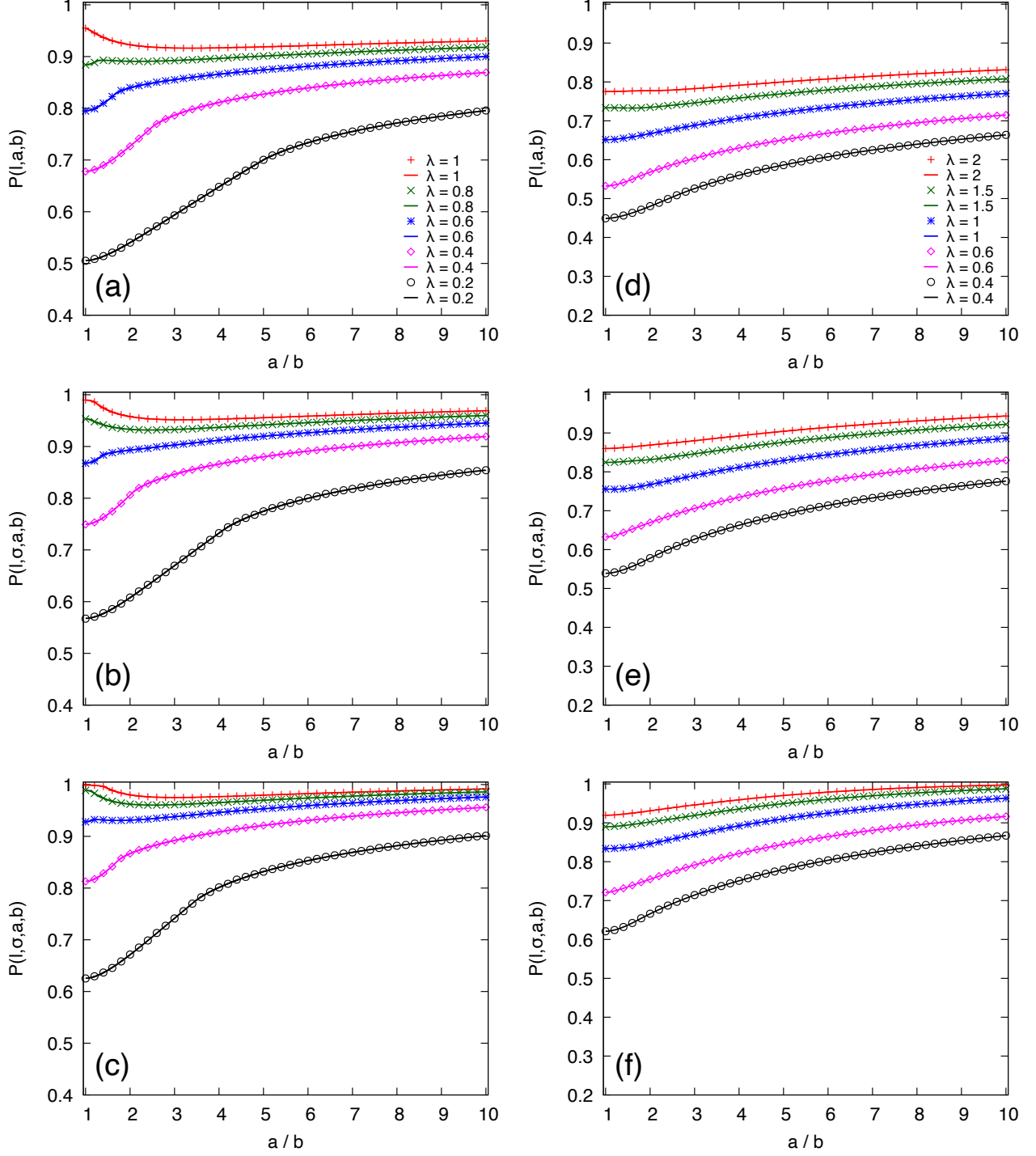


FIG. 5. Result of BLNP with needles and spherocylinders with fixed area ab of a grid cell. (a) The intersection probability $P(l, a, b)$ versus the ratio a/b is shown in the case of 2D needles. (b)-(c) The intersection probability $P(l, \sigma, a, b)$ versus a/b is shown in the case of 2D spherocylinders with $\sigma/l = 0.1$ and 0.2 , respectively. In each subfigure of (a)-(c), we show results when $\lambda = 1, 0.8, 0.6, 0.4, 0.2$. (d)-(f) Results are shown in the same format as (a)-(c), yet for the cases of 3D needles and spherocylinders. In each subfigure of (d)-(f), we show results when $\lambda = 2, 1.5, 1, 0.6, 0.4$. Each sign is from result of a single Monte Carlo simulation with $l = 3$ and a configuration size $N_{\text{all}} = 10^6$ for the 2D case and $N_{\text{all}} = 10^7$ for the 3D case. Lines are from analytical results.

ical approximation of an integral. In this section, we set $N_{\text{unit}} = 10^4$ and $\varepsilon = 10^{-9}$.

We first consider how the sizes of needles and spherocylinders affect an intersection probability. Fig.4 shows both results from numerical simulation and analytical theory. As we can see, an intersection probability increases monotonously with a larger length for a needle or a larger length and radius for a spherocylinder once the other size parameters are fixed. Besides, a comparison between Fig.4 (a)-(c) with (d)-(f) shows that, the introduction of a new degree of freedom for a dropped object generally pushes down intersection probability. The profile of intersection probability further changes drastically in the case of long objects: in the 2D cases, objects with a length beyond a finite critical value is sure to intersect with grid lines, while in the 3D cases only infinitely long objects intersect with grid lines with probability 1.

Based on Fig.4, we should mention that, in our equations of intersection probabilities there are four regions with different analytical forms. A naive extrapolation of an analytical form in a certain region to some region with a larger l only leads to an overestimation of intersection probability, until there is an unphysical result as the probability goes beyond 1.

From a different perspective, we further consider how an intersection probability evolves with the aspect ratio of grid cell a/b . This context is highly relevant when the BLNP is adopted as a physical model for filtration of particles through a grid, such as in literature of soft matter physics [5]. With our theory, we can locate those parameters leading to the maximal flux (correspondingly the minimal intersection probability), which can be further tested in a controlled experiment. We define a dimensionless control parameter $\lambda \equiv l^2/ab$, and calculate intersection probability with tuned λ . Given the control coefficient λ , the radius ratio σ/l ($\equiv \sigma_l$), and the aspect ratio a/b ($\equiv t$), a correspondence between parameters can be established as

$$\left(\frac{l}{a}, \frac{l}{b}, \frac{\sigma}{a}, \frac{\sigma}{b}\right) = \left(\sqrt{\frac{\lambda}{t}}, \sqrt{\lambda t}, \sigma_l \sqrt{\frac{\lambda}{t}}, \sigma_l \sqrt{\lambda t}\right). \quad (162)$$

Fig.5 shows both simulation and analytical result. Unlike the pattern of monotonously increasing intersection probability in Fig.4, we can find a much more complicated picture.

Results in Fig.5 (a)-(c) for 2D cases follow a quite similar pattern, as we can find a local minimum moving from $t = 1$ to some $t > 1$ with increasing λ . We present a possible qualitative scenario here: (1) when $\lambda \leq \lambda_1^*$, there is only one local minimum of intersection probability, which is exactly at $t_1 = 1$; (2) when $\lambda_1^* < \lambda \leq \lambda_2^*$, a second local minimum emerges at $t_2 > 1$, and a hump-like shape with a local maximum separates the two minima, yet the global minimal still happens at $t_1 = 1$; (3) when $\lambda_2^* < \lambda \leq \lambda_3^*$, the two local minima still coexists as in (2), yet the global minimum moves from $t_1 = 1$ to $t_2 > 1$; (4) when $\lambda_3^* < \lambda$, the local minimum at $t_1 = 1$ vanishes, and

the local minimum at $t_2 > 1$ becomes the global one. For Fig.5 (a), we test λ numerically and find that $\lambda_1^* \approx 0.771$, $\lambda_2^* \approx 0.830$, and $\lambda_3^* \approx 0.999$. An intuitive understanding of the scenario is that, with an increasing a/b and a grid cell becoming more elongated, there is a competition between a decrease in the intersection probability due to a larger width a and an increase in the intersection probability due to a smaller height b of the grid cell. Yet the dominant term in the competition simply depends on the control parameter λ . The above scenario of moving minimum is much like the one in the analysis of critical transitions and hysteresis with a stability landscape in a multiple stable system (see Fig.(2.6) in [18]), while the two minima here correspond to the two stable equilibrium states of the system and the control parameter λ acts as the strength of an external perturbation on the system.

Results in Fig.5 (d)-(f) for 3D cases follow a much more smooth way than those in the 2D cases. In most cases in Fig.5 (d)-(f), $t = 1$ is the global minimum for intersection probability. Yet we can still numerically find a different global minimum at $t > 1$. For example, in Fig.5 (d) for the case of 3D needles with $\lambda = 1.5$, we have $P(l, a, b) = 0.733559$ at $t = 1$ and a smaller $P(l, a, b) = 0.732816$ at $t = 1.605$.

For Fig.5, there still remains some fundamental questions, such as to theoretically ascertain the scenario of moving minimum in 2D cases, to analytically locate the global minimum with any given λ in the 2D cases, and to prove whether the results in the 3D cases still follow the scenario in the 2D cases. To fully resolve these questions, we need to carry out a detailed analysis of landscapes of intersection probabilities with respect to t . Due to the current amount of theoretical analysis and results in this paper, we would like to leave them to a future work.

VIII. CONCLUSION

Here we analytically study BLNP in different versions on their intersection probabilities. With a single probabilistic framework, we solve problem versions with dropped objects, with increasing analytical complexity, from a 2D needle with arbitrary length l to a 3D spherocylinder with arbitrary length l and diameter σ onto a grid with any width a and height b . Our analytical predictions are further validated by Monte Carlo simulation.

There are already many extensions of BLNP with physical backgrounds. Our analytical framework here, which applies to any size of needles and spherocylinders, helps to pave the way for principled theoretical approaches into untested parameter regions for these generalizations and variants.

ACKNOWLEDGEMENTS

This work is supported by Guangdong Major Project of Basic and Applied Basic Research No.

2020B0301030008, Guangdong Basic and Applied Basic Research Foundation (Grant No. 2022A1515011765), and National Natural Science Foundation of China (Grant No. 12171479).

-
- [1] Laplace P-S. *Théorie analytique des probabilités*. Paris: Veuve Courcier; 1812.
 - [2] Laplace P-S. *Théorie analytique des probabilités*. Third Revised Edition. Paris: Veuve Courcier; 1820.
 - [3] Buffon G-L. *Essai d'arithmétique morale*. *Histoire naturelle, générale et particulière, Supplément 1777*; 4: 46-123.
 - [4] Uspensky J V. *Introduction to Mathematical Probability*. New York: McGraw-Hill; 1937.
 - [5] Dell Z E, Franklin S V. The Buffon-Laplace needle problem in three dimensions. *J Stat Mech* 2009; P09010.
 - [6] Diaconis P. Buffon's Problem with a long needle. *J Appl Prob* 1976; 13: 614-8.
 - [7] Barbier E. Note sur le problème de l'aiguille et le jeu du joint couvert. *J Math Pur App* 1860; 5: 273-86.
 - [8] Ramaley J F. Buffon's Noodle Problem. *Am Math Mon* 1969; 76: 916-8.
 - [9] Johannesen I G. The Buffon needle problem revisited in a pedagogical perspective. *Math J* 2009; 11: 284-99.
 - [10] Basel U. Buffon's problem with a pivot needle. *Elem Math* 2015; 70: 67-70.
 - [11] Chung C F. Application of the Buffon Needle Problem and its extensions to parallel-line search sampling scheme. *Math Geo* 1981; 12: 371-90.
 - [12] Zhang S. The exact power law for Buffon's needle landing near some random Cantor sets. *Rev Mat Iberoam* 2020; 36: 537-48.
 - [13] Vardakis D, Volberg A. The Buffon's needle problem for random planar disk-like Cantor sets. *J Math Anal Appl* 2024; 529: 127622.
 - [14] Godréche C. The Buffon needle problem for Lévy distributed spacings and renewal theory. *J Stat Mech* 2022; 013203.
 - [15] Duma A, Stoka M. Hitting probabilities for random ellipses and ellipsoids. *J Appl Prob* 1993; 30: 971-4.
 - [16] Landau D P, Binder K. *A Guide to Monte Carlo Simulations in Statistical Physics*. Fourth ed.. Cambridge: Cambridge University Press; 2015.
 - [17] Press W H, Teukosky S A, Vetterling W T, Flannery B P. *Numerical Recipes: The Art of Scientific Computing*. Third ed.. Cambridge: Cambridge University Press; 2007.
 - [18] Scheffer M. *Critical Transitions in Nature and Society*. Princeton: Princeton University Press; 2009.